Sudan University of Science and Technology

College of Graduated Studies

Mechanical Engineering Department

Aerodynamic analysis of (GRAD)Rocket using (CFD)

تحليل الديناميكا الهوائية للصاروخ (GRAD) باستخدام ديناميكا الموائع التحسيبية

Partial fulfilment of the Requirements for the degree of Master of Science in Mechanical Engineering (Power)

By

Ammar Eltaj Mohammed Ahmersheen

BSc. Omdurman Islamic University 2013

Supervisor

Dr. Sakhr Babikir Hassan AbuDarag

June 2019

Dedication:

Dedicated to:

My great mother

The spirit of my father

My family

My friends

Acknowledgment

Thanks and appreciation to Supervisor **Dr. Sakhr Abu Darag** for his assistance, guidance, encouragement and cooperation during the research period.

Thank you very much to the members of the teaching staff of the Sudan University of Science and Technology and thanks also to the members of the Mechanical Engineering School.

I would also like to extend my sincere thanks to **SMT**, Marbel Engineering Company for the great assistance in providing the laboratory and equipment needed and providing consultancy to complete the research.

Abstract

In this research, The aerodynamic coefficients and stability derivatives for supersonic (GRAD)rocket in active and passive phases have been calculated. The modifications have been implemented are ogive nose shape and increased in fins number. The impacts of fins configuration and setting angle have been also demonstrated. The Computational Fluid Dynamics and Missile Datcom are used in the simulation.

The study has adopted three different configurations of WAFs for rocket and single domain technology to investigate the lateral and rolling characteristics of WAFs, including the fins setting angles. Simulation has been performed at Mach numbers ranging from 0.4 to 3 through angle-of-attack and side slip angle from zero to 9 degree.

The result represents that the wrapped around fins (WAF) configuration is greatly improved the longitudinal stability and enhanced the longitudinal aerodynamic characteristics for the rocket. The total drag of the rocket is mainly stemmed from the body, while the drag generated by the WAF account for only about 18.45 per cent.

Maintaining negative fins setting angle is provided additional side and rolling moments which enhanced lateral and longitudinal stability. Both, lateral and longitudinal stability are investigated.

Simulation captured Shock wave at missile's nose and fins, and represented the flow properties around missile configuration.

The Missile Datcom software was used to verify and validate the CFD's results and the results comparison showed satisfactory agreement between the two different solutions.

المستخلص

فى هذا البحث تم حساب المعاملات الأيروديناميكية ومشتقات الاستقرارية للصاروخ (GRAD) ذوالسرعة فوق الصوتية في حالة وجود دفع من المحرك النفاث وفى حالة عدم وجود دفع من المحرك النفاث. التحديثات التي تم تنفيذهاعلى الصاروخ هي شكل المقدمة المماسي وزيادة عدد الاجنحة. كما تم توضيح تأثيرات شكل الاجنحة وزاوية وضع الاجنحة. وتم استخدام ديناميكا الموائع الحسابية (Ansys/Fluent) وبرنامج (Missile Datcom) في المحاكاة.

اعتمدت الدراسة ثلاثة نماذج من الاجنحة المعكوفة (WAFs) بزوايا انحراف مختلفة 0.5-، 0.0،0.5، وتكنولوجيا Single domain للتحقق من المعاملات الأيروديناميكية ومشتقات الاستقرارية للصاروخ معكوف الاجنحة ، . تم إجراء المحاكاة عند ظروف تشغيلية لرقم Mach يتراوح من 0.4 إلى 3 خلال زاوية الهجوم وزاوية الانزلاق الجانبية من صفر إلى 9 درجة.

تعرض النتائج أن الاجنحة المعكوفة الشكل (WAFs) تحسن بشكل كبير من الاستقرارية الطولية وتعزز الخصائص الايروديناميكية الطولية للصاروخ. تتبع الاعاقة الكلية للصاروخ بشكل أساسي من الجسم ، بينما يبلغ مقدار الاعاقة الناتج عن الاجنحة المعكوفة (WAFs) حوالي 18.45 في المائة فقط.

الابقاء على زاوية وضع الاجنحة السالبة يولد عزم جانبي وعزم دوران والذي بدوره يحسن الاستقرارية الجانبية والطولية للصاروخ. كما ، تم التحقيق الاستقرار الجانبية والطولية.

كما يعرض البحث صور للجريان حول الصاروخ وتم التقاط صور للموجات الصدمية عند مقدمة الصاروخ وعند الاجنحة وتم عرض بعض خصاص الجريان حول الصاروخ.

تم استخدام برنامج(Missile Datcom) للتحقق من صحة نتائج (CFD) ،وأظهرت مقارنة النتائج اتفاقًا مرضيا بين الطريقتين المختلفتين.

Table of contents

List of symbols

symbol	Description	unit
S_{ref}	Reference Area	m^2
C_r	Root chord	m^2
C_{tip}	Tip chord	m^2
b	Wing span	m
D	Body diameter	m
L	Total length	m
p	Pressure	Pas
AOA	Angle of attack	Degree
M	Mach number	Dimensionless
AR	Aspect ratio	Dimensionless
C_l	lift coefficient	Dimensionless
C_D	Drag coefficient	Dimensionless
C_z	Side force coefficient	Dimensionless
C_{mz}	Pitch moment coefficient	Dimensionless
C_{my}	yaw moment coefficient	Dimensionless
C_{mx}	roll moment coefficient	Dimensionless

List of abbreviations

Abbreviations	Description
CFD	Computational Fluid Dynamics
MD	Missile Datcom
WAF	Wrapped Around Fin
6DOF	Six Degree Of Freedom
DNS	Direct Numerical Simulation
RANS	Reynolds-Averaged Navier-Stokes
CPU	Central Processor Unit
SRS	Scale-Resolving Simulation
LES	Large Eddy Simulation
S-A	Spalart-Allmaras
EWT	Enhanced Wall Treatment
SMT	Sudan Military Technology

Greek symbols

Symbol	Description
α	Angle of attack
β	Side slip angle
δ	Setting angle
ω	Specific rate of dissipation
ε	Turbulence dissipation rate
ρ	density

Chapter 1:

INTRODUCTION

1.1 General Introduction:

A rocket is defined as a missile or a vehicle that generates thrust from a rocket engine [1]. The engine exhaust of the Rocket is formed entirely from propellant carried by rocket body. Rocket engine operates by action and reaction and push rockets forward according to Newton's second law theory [2]. To control the flight, rockets utilize many parameters such as momentum, airfoils, auxiliary reaction engines, thrust, propellant flow, spin and gravity. Rockets for military uses refer to at least 13th century, whereas for civilian use did not occur until the 20th century [3]

As a result of highly cost of experimental investigation (wind tunnel experiment) in developing Rockets performance, the simulation programs has become very important as a preliminary design tool in various engineering application. Moreover, determination of aerodynamic forces and moments coefficients using classical methods is difficult and it is not precise enough especially for complicated geometries and high speed regions.

Developed CFD techniques are considered as modern methods that have been used to determine and validate the aerodynamic quantities of flying objects, and ANSYS, FLUENT software is a one of these tools with fully capability to simulate and determine many applications. In this project this software has been used to simulate and determine the aerodynamic coefficients for GRAD developed rocket.

GRAD rocket is at present the weapon system that is mostly equipped and widely used all over the world (approximately fielding in over 30 countries). It is priority to use this methodology for determination of aerodynamic forces and moment coefficients to be used later as a basic data in other applications such as the design of guidance and control system, and preparing firing tables.

1.2 Scope of the Research:

Use computational fluid dynamics (CFD) techniques to calculate the aerodynamic coefficients and stability derivatives for supersonic GRAD developed rocket.

1.3 problem definition:

As a result of continuous development of defense products and to keep abreast of the developments in military technology, there is a need to develop many of the existing products in the service. The product GRAD rocket is one of these products which, has conical nose shape and four wrapped around fins and it reaches 20km maximum range. This project aims to calculate the aerodynamic coefficients for Developed GRAD rocket with new modifications in the geometry such as, the tangent ogive nose shape and six wrapped around fins. These aerodynamic coefficients are considered as inputs data for other applications such as design of guidance and control system, preparing firing tables and trajectory calculations.

1.4 Layout of the Project:

Chapter one is purely introductory in character, chapter two collects previous studies related to the research problem, chapter three represents the Computational Fluid Dynamic steps which applied to the research case study, chapter four shows the results and discussions of the simulation and results validation, and last chapter indicates research conclusions and recommendations for future studies.

1.5 Methodology:

In this research, the aerodynamics parameters of GRAD developed were calculated. Horizontal measurements have been performed for the missile with two prepared geometries, full and empty propellant. Both of the models were set up with different deflection angles against range of angle of attack and range of side slip angle.

After geometries are prepared, mesh and boundary conditions were set up in GAMBITE software and the mesh was exported to ANSYS FLUNT. Flight conditions, operation conditions and turbulence model were defined. The appropriate method for the solution was selected and the simulation was executed. The results of CFD method obtained have been analyzed and validated using Missile Dotcom software.

1.6 Objectives:

This project aims to simulate and determine the aerodynamic coefficients for GRAD develop rocket using CFD method. The study covered the following tasks:

- Determination of the aerodynamic force and moment coefficients for the GRAD develop rocket regarding to different Mach number and angle of attack.
- Study the static stability for both full load and empty load for the existing model .
- Analysis the effect of the static stability margin regarding to Mach number and angle of attack.

- Study the dynamic stability derivatives for the existing model with different Mach numbers and determine the recommendations for further development.

Chapter 2:

LITERATURE REVIEW

2.1 Background studies:

The development of supersonic GRAD rocket has been covered by extensive research during last twenty years. For example, Slobodan *et al*. [4] were measured the rolling moment coefficients for two models with wraparound fins and one model with flat fins. The rolling moment coefficients were measured for two cant angles (0^o and 0.8^o). The measured values were fitted by the fourth order polinom of the angle of attack. It was proven that the rolling moment coefficient at zero angle of attack is equal to the sum of the rolling moment coefficient due to the curvature of the fins and rolling moment coefficient of the canted equivalent flat fins. They obtained the flat fins by projected the wraparound fins on the plane through longitudinal axis and root chord of the wraparound fins. They proved by the measurements of the rolling moment coefficient that the rolling moment coefficient is an even function of the angle of attack. The rolling moment coefficient is expressed in the form of Fourier's series in the aerodynamic axis system.

Ravi Krishna *et al* [5], were represented the results of a numerical study to understand the flow field over a projectile with wraparound fins. This investigation is performed in order to determine aerodynamic coefficients for the missile model for varying Mach number from 1.2 to 2.5. The roll moment coefficients were computed from the flow field solution and compared with other computational models and experimental works. The results show a reversal of the rolling moment in a Mach number from 1.2 to 1.4. While generating Mach number profile along missile body, a transition from subsonic to supersonic flow was notably found just before the fin-tip in the Mach number range from 1.2 to 1.4. This transition from subsonic to supersonic just before the fin seems to be the main cause for the roll reversal, which makes the flow inside the fin passage behave differently.

Furthermore, it was seen that most of the effect was confined towards the leading edge of the fins.

Also Attapon, *et al* [6] were introduced a new way to find the aerodynamic characteristic equation of missile for the numerical trajectories prediction more accurate. The goal is to obtain the polynomial equation based on two missile characteristic parameters, angle of attack and flight speed. First, the understudied missile is modeled and used for flow computational model to compute aerodynamic force and moment. Using commercial CFD software to solve flow simulation with tetrahedron elements and the boundary conditions are specified by two variables velocity and angle of attack. The equations are formed by curve fitting data obtained from simulation. The equations were constructed in form of perpendicular force, axial force and moment which depended on two variable parameters, velocity and angle of attack and the obtained equation has power 3 of velocity term as we expected and corresponded with the classical aerodynamic theory.

Moreover F. MINGIREANU *et al* [7] were conducted a full 6 DOF modeling for a GRAD rocket in Earth's non-inertial frame. For numerical purposes the modeling is limited to flat Earth approximation. The full motion equations are shown and all terms are explained together with the aerodynamics parameters for the entire flight envelope. Non-linear interpolation is used for aerodynamic coefficients and their derivatives. the presented the typical dispersion factors due to rocket production inaccuracies, launch condition variability and atmospheric factors and their relative influence on a guidance implementation package. Next they presented a 6 DOF modeling with various step-like thrust-curves while maintain the same total impulse delivered by the original motor. The influence of the step size on the range of the GRAD rocket is investigated together with the dispersion influence. They showed that significant range increase can be obtained while using the same propulsion unit

with a step-like thrust-curve modification. We also investigate the influence of the step-like thrust-curve on dispersion of such a rocket and the technological possibilities to implement our solution. In the last part of the paper we present a terminal guidance concept 122 mm rockets. A preliminary requirement for IMU units to be used for terminal guidance is shown together with the general guidance algorithm for several trajectories. Performance expectations are shown through the analysis of the IMU units performance as well as flight dynamics of the 122 mm rockets.

In addition, Chun-Chi Lia, *et al* [8] studied integrated a low-speed wind tunnel experiment, CFD, and MATLAB/Simulink to analyze the aerodynamic attributes and simulate flight trajectories of a tail fin-stabilized projectile with two shapes. The Karman-Tsien rule was used to revise and convert the air compressibility of the low-speed wind tunnel trial data into subsonic wind tunnel 0.6 Mach data, which could subsequently reduce costs. The results of two types of projectiles showed that the aerodynamic coefficients CD, CL, CM and CMα of the converted experiment data were similar to the computational data within an angle of attack within +/-8°. Results for both the trail experiments and CFD showed that two types of projectiles possessed excellent aerodynamic attributes and maintained flight stability within an angle of attack of -8° and 8°. Compare two types of projectiles launched at a 45°(800 mil) in elevation, the improved type (model B) increased 26.83% range distance than prototype (model A). This indicates that by integrating wind tunnel experiments, CFD, and MATLAB/Simulink, an economic method to design aerodynamic systems, analyze and compare flow fields, and simulate flight trajectories for field testes can be established.

Beside this, Guo Qing, Zhang et al [9] were investigated the aerodynamics characteristics (especially the side force/moment and rolling characteristics) to

analyze the impacts generated by different parameters of wrap-around fins (WAFs) and to find the corresponding mechanism. Design/methodology/approach – The paper has adopted three different types of WAFs for the rocket configurations and the sub-regions divided technology to investigate the lateral and rolling characteristics of WAFs, including the fins with variations in span to chord ratio, thickness, leading-edge sweep, curvature radius, fin numbers, setting angles and rotated angles. Simulations have been performed at Mach numbers from 3 to 4 through an angle-of-attack range of about 0° to 10° and at model rolling angles of 45° to 90°. Findings – The paper shows that the WAF configurations can greatly improve the longitudinal stability and enhance the longitudinal aerodynamic characteristics for the whole rocket. The total drag of the whole rocket is mainly stemmed from the body, while the drag generated by the WAF account for only about 7.42 per cent. The extra side forces and rolling moments are due largely to the unequal pressure distributions on both sides of the fin (windward or leeward). Maintaining a certain negative setting angle, δ, can effectively avoid the coning movement and improve the flight stability at high angles of attack. The size of the span and chord are two main factors in controlling the longitudinal characteristics. For the side force/moment and rolling characteristics, different geometric parameters of the WAFs have played different roles. Originality/value – The paper provides the qualitative and quantitative analysis for different WAFs configurations by investigating the curves of different parameters and contouring of static pressure distributions. Findings can provide some suggestions for the designers for avoiding some significant dynamic problems, such as Magnus instability and roll rate variations during flight.

Chapter 3:

MODELING & SIMULATION

3.1 Introduction:

Computational fluid dynamics (CFD) is the analysis of systems involving fluid flow, heat transfer and associated phenomena such as chemical reactions by means of computer-based simulation. The technique is powerful and spans a wide range of industrial and non-industrial application areas [10].

The availability of affordable high performance computing hardware and introduction of user friendly interfaces have led to a recent upsurge of interest and CFD poised to make an entry into the wider industrial community in the 1960s [7].

Aerodynamic is an applied science with many practical applications in engineering. The prediction of forces and moments and heat transfer to bodies moving through a fluid is a one of aerodynamic practical objectives.

The aerodynamic forces and moments produced on a missile by its motion through the air affect every other field involved in the design of guide missile such as (structure, control system, propulsion).

The aerodynamic design of airfoil sections continues today as an elegant yet practical engineering design problem. It is elegant in that the solution of any airfoil design problem, however complex, is nothing more than a two-dimensional closed contour. It is practical in that many, if not most, problems in aerodynamics involve the generation of lift, drag, and moment by airfoil sections [11].

Determination of aerodynamic forces and moments coefficients using classical methods is difficult and it's not precise enough especially for complicated geometries and high speed regions.

CFD is a one of the modern methods that has been used to determine and validate the aerodynamic quantities of flying objects, and ANSYS, FLUENT

software is a one of these tools with full capability to simulate and determine many applications, but in this project it will be used to simulate and determine the aerodynamic coefficients for GRAD develop rocket.

3.2. Missile Aerodynamics versus Airplane Aerodynamics:

One of the principal differences between missiles and airplanes is that the former are usually expendable, and, consequently are usually uninhabited. For this reason, increased ranges of speed, altitude, and maneuvering accelerations have been opened up to missile designers, and these increased ranges have brought with them new aerodynamic problems. For instance, the higher allowable altitudes and maneuvering accelerations permit operation in the nonlinear range of high angles of attack. A missile may be ground-launched or air-launched and in consequence can undergo large longitudinal accelerations, can utilize very high wing loadings, and can dispense with landing gear. In the absence of a pilot the missile can sometimes be permitted to roll and thereby to introduce new dynamic stability phenomena. The problem of guiding the missile without a pilot introduces considerable complexity into the missile guidance system. The combination of an automatic guidance system and the air frame acting together introduces problems in stability and control not previously encountered. Many missiles tend to be slender, and many utilize more than the usual two wing panels. These trends have brought about the importance of slender-body theory and cruciform aerodynamics for missiles [12].

3.3 Computational fluid dynamic methodology:

Computational Fluid Dynamics (CFD) process is the steps to set up a problem and run the code. For CFD exercise, two software have been used: Firstly, GAMBIT software is used for pre-processing stage (prepare and clean up

the geometry, generate mesh and set up the boundary conditions). Secondly, Fluent software is used for processing and post-processing (solution and results). Figure3.1shows Computational fluid dynamic steps.

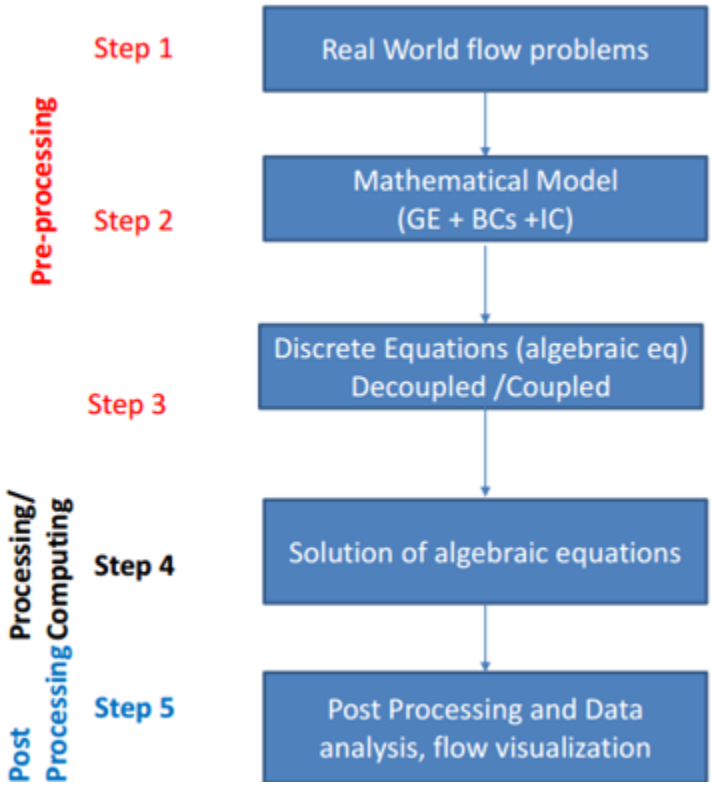

Figure 3.1: Computational fluid dynamic steps

3.3.1 Geometry preparation:

The geometry of the missile is prepared after horizontal measurements of the missile and three different geometries of *Wrap Around Fins* (WAFs) rocket configurations are considered. Simulations are performed at Mach number from 0.4 to 3 through an angle-of-attack range of 0° to 9° and at fins setting angles (+0.5,0,-0.5) degree by adopting the single domain technology.

The geometry of the rocket is mainly composed of two parts:

1. **Body**: With the large length-diameter ratio, it can also be divided into four parts: head, middle body, fin body and back body.
2. **Fins:** With six wrapped fins distributed evenly on the body circumference all fins are identical in span, chord, thickness, leading-edge sweep angle and setting angle.

The dimensions of the missile are represented as a function of the missile caliber and The geometric parameters of the WAF missile model considered are shown in figures 3.2.a,b,c

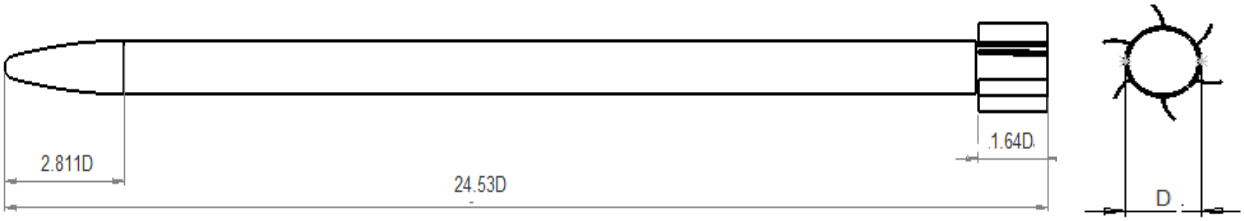

Figure 3.2.a: Geometry configuration and dimension

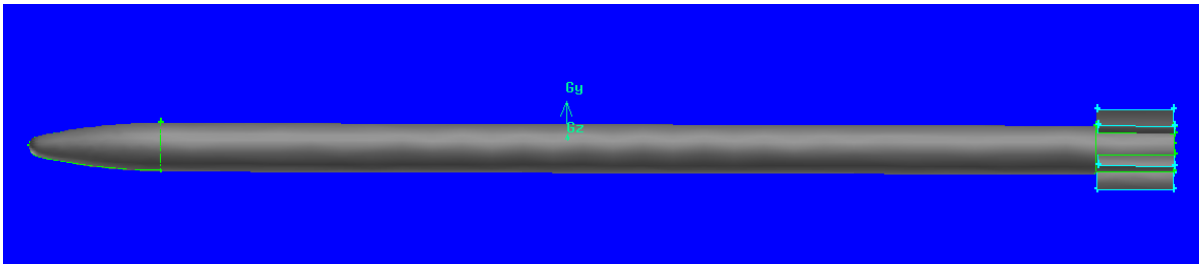

Figure 3.2.b: Computational geometry configuration

Figure 3.2.c: Real geometry configuration [13]

3.3.2 Computational mesh:

Before generating numerical solution into the partial differential equations form that governs fluid flow, the physical flow domain must be discretized. This discretization may be based on structured and unstructured concept.

In a structured grid, points are arranged so that their relative positioning in physical space is preserved in their computational storage; i.e., point adjacent to a given point in physical space is also adjacent in computational space. On the other hand, there is not necessarily any correspondence between a points physical and computational neighbors in unstructured grids [11].

The method of single domain technology is used and the domain is divided to fixed domain (near to the missile's body) which is more refined mesh and deformed domain.

The mesh size of the missile surfaces was small because the missile body is an area of interest so the mesh should be refined. Figure 3.3 shows missile surfaces mesh.

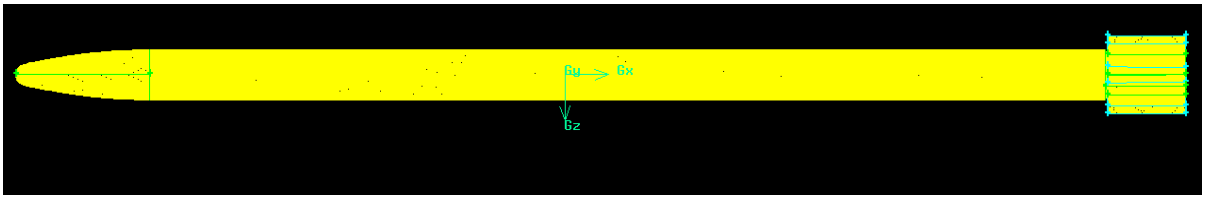

Figure 3.3: Missile surfaces mesh

The small domain around missile mesh is refine and it used to make mesh near the missile body is refine more than the area far away from the missile body, so the mesh size starts to increase gradually because the surfaces of this volume represents the source of the size function that used to generate gradual mesh increment to the region far away from the missile body. Figure3.4 shows small domain mesh.

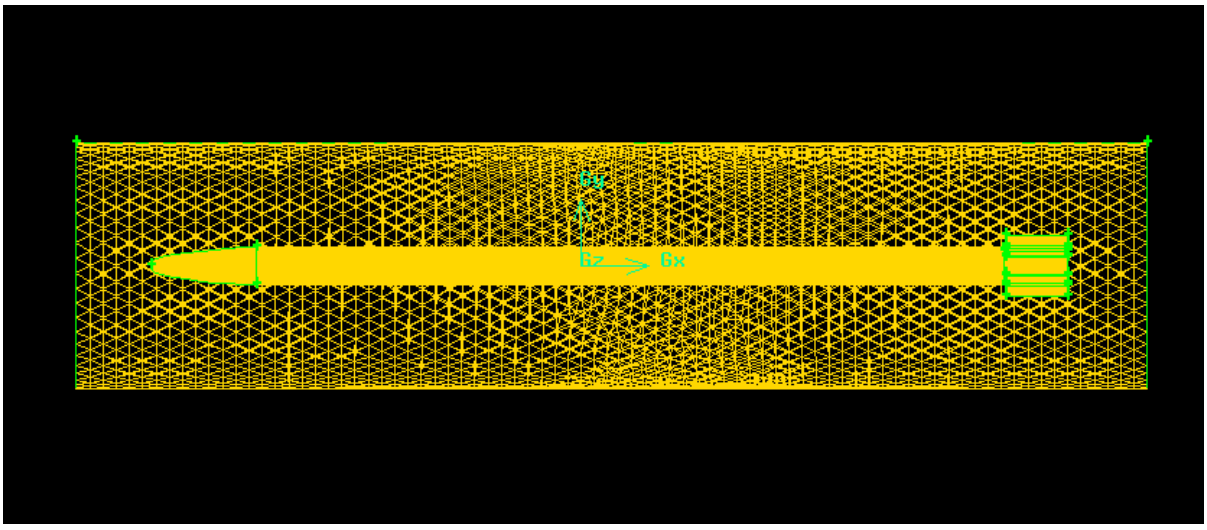

Figure 3.4: Small domain mesh

Size function option is used to generate mesh for total computational domain and the mesh generated without skewness problem and the mesh is refined near to the missile's body as shown in figure 3.5.

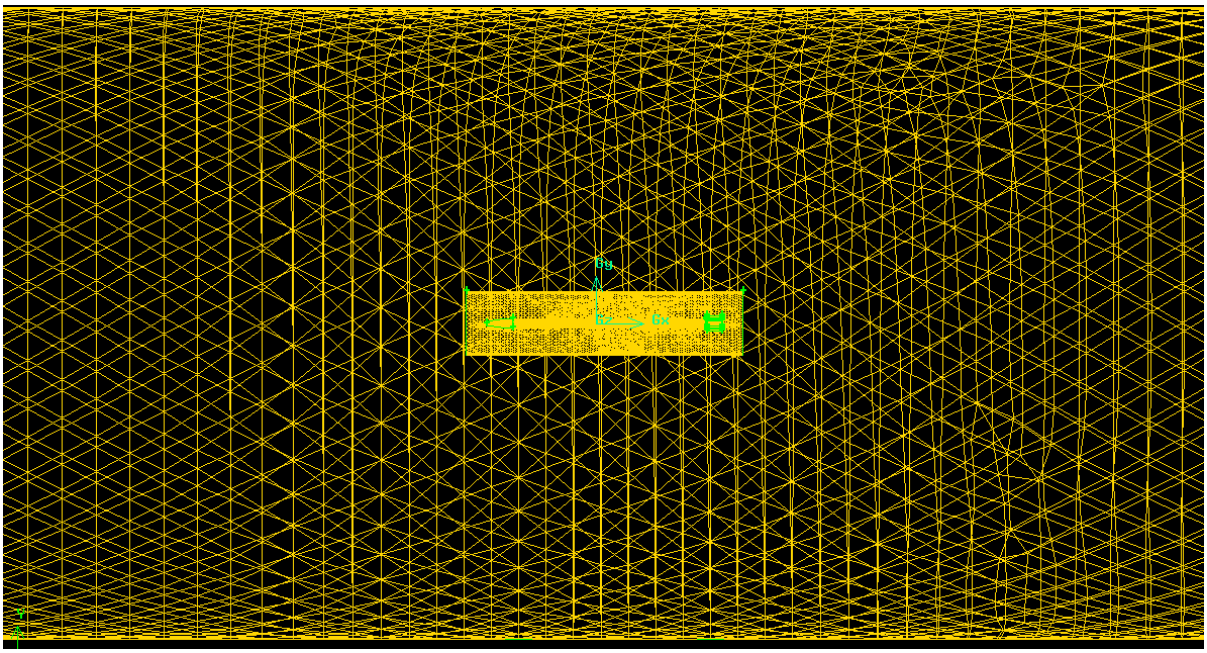

Figure 3.7: External computational domain mesh

Figure3.6 shows the mesh around fins and close to the missile's body and nose ,which they represent the areas of interest .

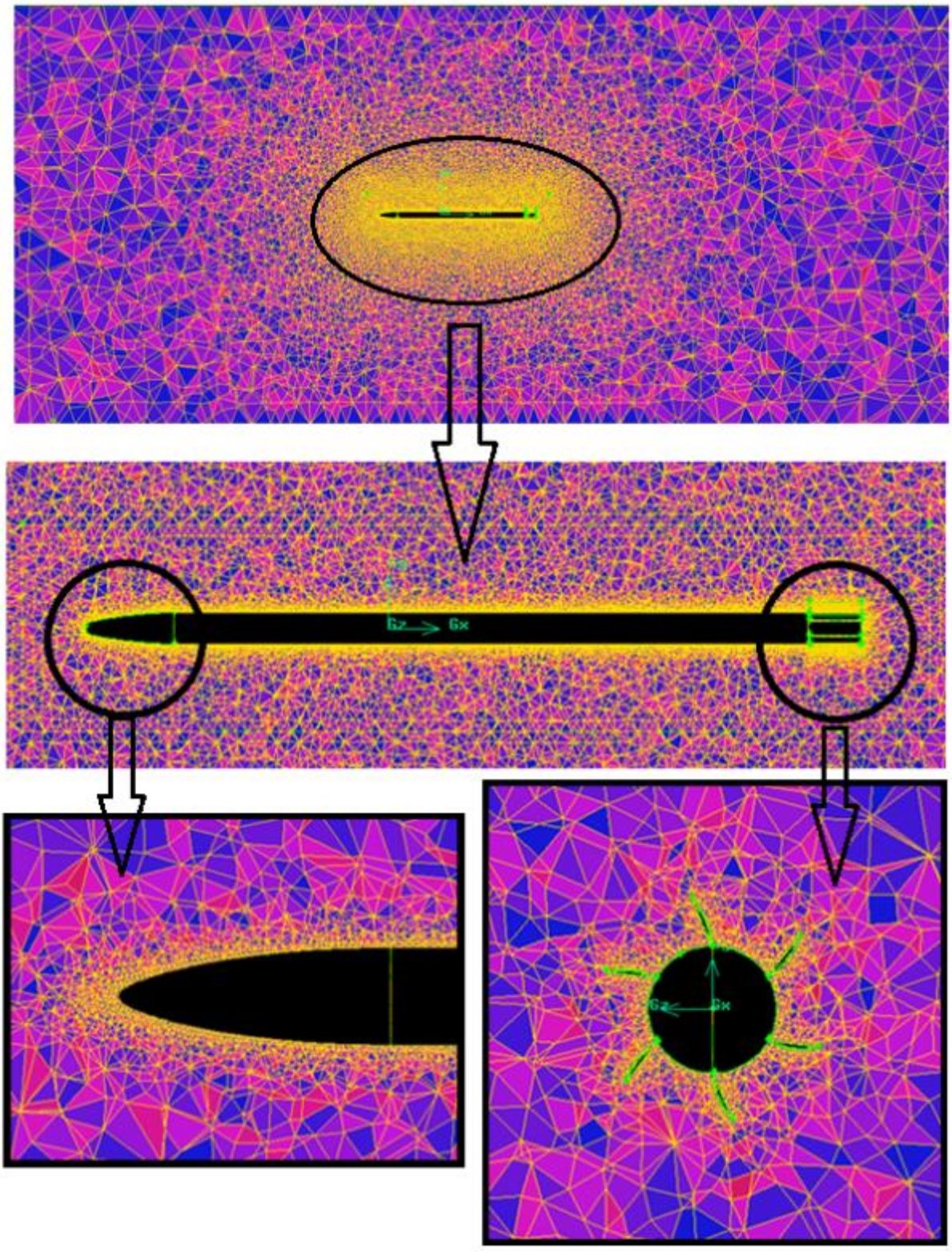

Figure 3.8: Mesh is refined close to the missile's body and fins

3.3.3 Domain and Number of Elements:

The domain has been created to be far away from the missile to ensure that the boundaries of domain do not affect on the flow around the body of the missile The number of mesh element was1,547073element for different geometries.

3.3.4 Set up the Boundary Conditions:

Table 3.1 The boundary conditions are set up according to the following table:

Boundary	**Description**	**Type**
Back-face	Close surface at the end of the object	wall (in case of passive phase) mass flow rate(in case of active phase
Far	The domain of flight	Pressure far field
Wing	Fins of missile	Wall
Body	missile body	Wall
Interior	Face between fixed & modified volumes	Interior

3.4 Mathematical Models:

The governing equations of compressible Newtonian fluid flow are:

$$\text{Mass:} \quad \frac{\partial \rho}{\partial t} + \nabla \cdot (\rho \mathbf{u}) = 0 \quad \text{.....3.1}$$

$$x-\text{momentum:} \quad \frac{\partial (\rho u)}{\partial t} + \nabla \cdot (\rho u \mathbf{u}) = -\frac{\partial p}{\partial x} + \nabla \cdot (\mu \nabla u) + S_{Mx} \quad \text{.....3.2}$$

$$y-\text{momentum}: \quad \frac{\partial(\rho v)}{\partial t}+\nabla\cdot(\rho v\mathbf{u})=-\frac{\partial p}{\partial y}+\nabla\cdot(\mu\,\nabla v)+S_{My} \quad \text{.....3.3}$$

$$z-\text{momentum}: \quad \frac{\partial(\rho w)}{\partial t}+\nabla\cdot(\rho w\mathbf{u})=-\frac{\partial p}{\partial z}+\nabla\cdot(\mu\,\nabla w)+S_{Mz} \quad \text{.....3.4}$$

$$\text{Internal energy}: \quad \frac{\partial(\rho i)}{\partial t}+\nabla\cdot(\rho i\mathbf{u})=-p\,\nabla\cdot\mathbf{u}+\nabla\cdot(k\,\nabla T)+\Phi+S_i \quad \text{.....3.5}$$

Equations of state: $p=p(\rho,T)$ and $i=i(\rho,T)$

e.g. for perfect gas : $p=\rho RT$ and $i=C_vT$ 3.6

3.5 k-ω SST turbulence Model:

has been designed to avoid the freestream sensitivity of the standard k-ω model, by combining elements of the ω- The **SST k-ω** model equation and the ε-equation. In addition, the SST model has been calibrated to accurately compute flow separation from smooth surfaces. Within the k-ω model family, it is therefore recommended to use the SST model. The SST model is one of the most widely used models for aerodynamic flows. It is typically somewhat more accurate in predicting the details of the wall boundary layer characteristics uses the enhanced wall treatment as default .

The transport equations of The **SST k-ω** model can be written as:

$$\text{kinetic energy}: \quad \frac{\partial(\rho k)}{\partial t}+\frac{\partial(\rho k u_i)}{\partial x_i}=\frac{\partial}{\partial j}(\Gamma_k\frac{\partial k}{\partial x_j})+G_k-Y_k+S_k \quad \text{.....3.7}$$

Where:

$$G_k=\mu_t S^2 \quad \text{,and } S\equiv\sqrt{2S_{ij}S_{ij}} \quad \text{.....3.9}$$

$$Y_M=2\rho\omega M_t^2 \text{ and } M_t=\sqrt{\frac{k}{\gamma RT}} \quad \text{.....3.10}$$

specific dissipation rate: $\frac{\partial(\rho\omega)}{\partial t} + \frac{\partial(\rho\omega u_i)}{\partial x_i} = \frac{\partial}{\partial x_j}(\Gamma_\omega \frac{\partial \omega}{\partial x_j}) + G_\omega - Y_\omega + D_\omega + S_\omega$.....3.11

$\Gamma_k = \mu + \frac{\mu_t}{\sigma_k}$.....3.12

$\Gamma_\omega = \mu + \frac{\mu_t}{\sigma_\omega}$.....3.13

$\mu_t = \alpha^* \frac{\rho k}{\omega}$.....3.14

3.6 solution strategy:

Density based solver with implicit formulation was used and The velocity formulation was chosen to be absolute and Least Square Cell-Based gradient option was used. The fluid used for flow field was taken as air with properties of ideal gae,. Operating condition was set as standard see level conditions for the simulation work. The discretization of momentum equation, energy equation and conservation equation was done using second-order up-winding scheme.

Aerodynamic forces and moments were monitored at each iteration to figure out the solution convergence and solution stability.

Turbulence computational fluid dynamics simulations were performed in SMT's high performance computing system (Super Computer) and parallel CPUs were used for this study. The simulations were done with a maximum Courant number of 5 for all Mach number. In case of high angle of attack and high speed the simulation was started with low Courant number value of 1 and ramped up to the maximum value during the iterations of the simulation and Solution was converged more than 9,000 iterations depending on the Mach number, angle of attack and geometry. The convergence was determined by tracking the change in the flow

residual and the aerodynamic coefficient plots stability during the solution as shown in figure 3.9.

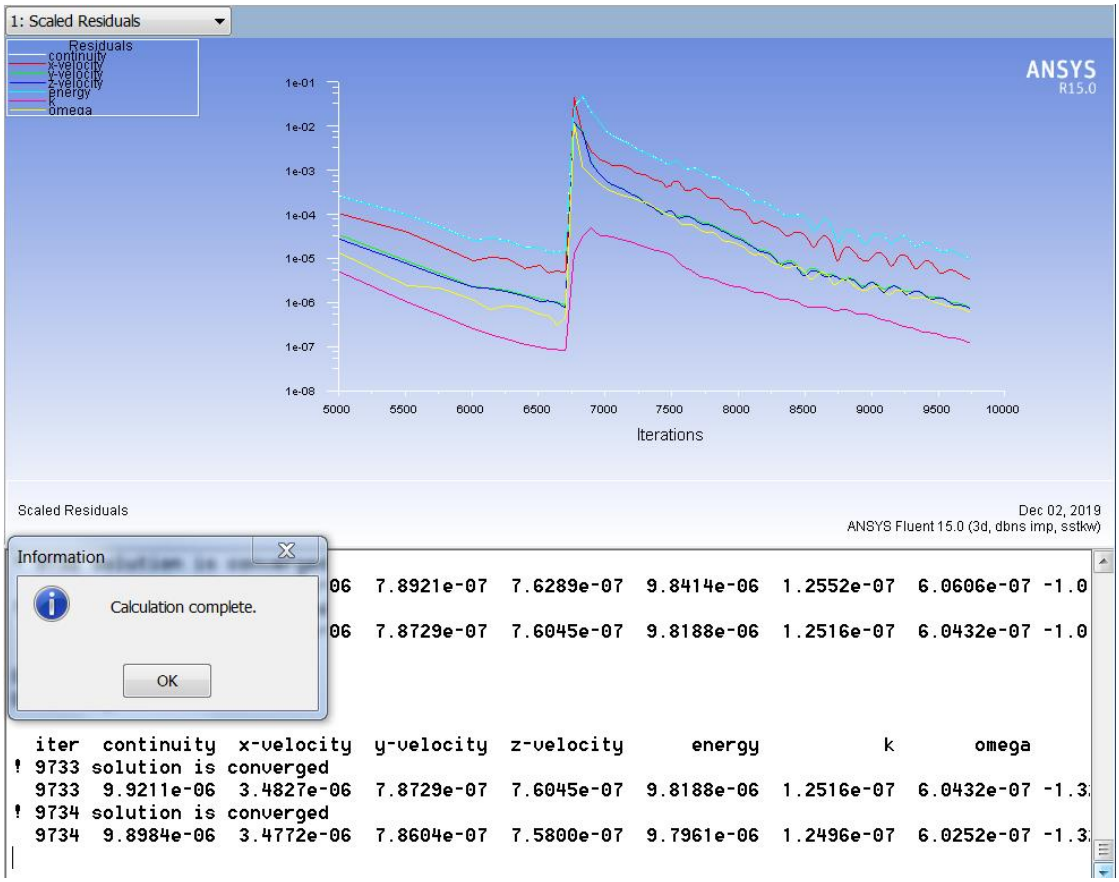

Figure 3.9: flow residual and convergence tracking

3.7 Introduction to Missile Datcom (MD) software:

Missile Datcom Software (MD) is an in-house software tool (closed source) used with a powerful concept during conceptual and preliminary design stages with advantages of short period and economical behavior regarding to the other methods.

Missile Datcom software is a widely used semi-empirical datasheet component build-up method to calculate the aerodynamic force and moment coefficients, static and dynamic stability derivatives and the trim condition of the flying objects (standard bodies) for zones from subsonic to hypersonic speed [18].

Chapter 4:

RESULTS & DISCUSSINOS

4.1 Introduction:

The simulation for both, Active and Passive phase of Missile have been performed for range of Mach number $0.4 \leq M \leq 3$ and different deflection angles $-0.5 \leq \delta \leq 0.5$ versus angle of attack $0 \leq \alpha \leq 9$, through side slip angle $0 \leq \beta \leq 9$. Super computer is utilized with more than 5,000 iterations to converge the solution. Thereafter, the aerodynamic properties and derivatives were recorded and analyzed. To confirm and validate the results, the Missile Datcom software (MD) is used.,

4.2 Results validation:

To verify the results, the simulations were carried out for two missile models. The first model represents the cylindrical body of finless missile, and the second one represents the rocket body with fins.

This classification is considered because this type of missiles has wrapped wings, and it is difficult to define the wrapped fins in Missile Datcom program. The program deals only with planar fins of standard shapes, which considered as one of the limitations of this technique.

The Missile Datcom program understands the wrapped fins as flat fins when it called from its library and then starts the calculation of the aerodynamic coefficients. Therefore, a slight difference in results is observed between the analytical and computational solutions.

The technique used to verify and confirm the results of the **CFD** method with **MD** program, is considered the cylindrical body of the missile without fins as first model and run the both software for subsonic and supersonic regions with Mach numbers 0.8 and 4.0 respectively for passive phase missile model.

The results reveal satisfactory agreement between the two solutions in both high subsonic region and supersonic flow region as shown in Figure (4.1.a,b).

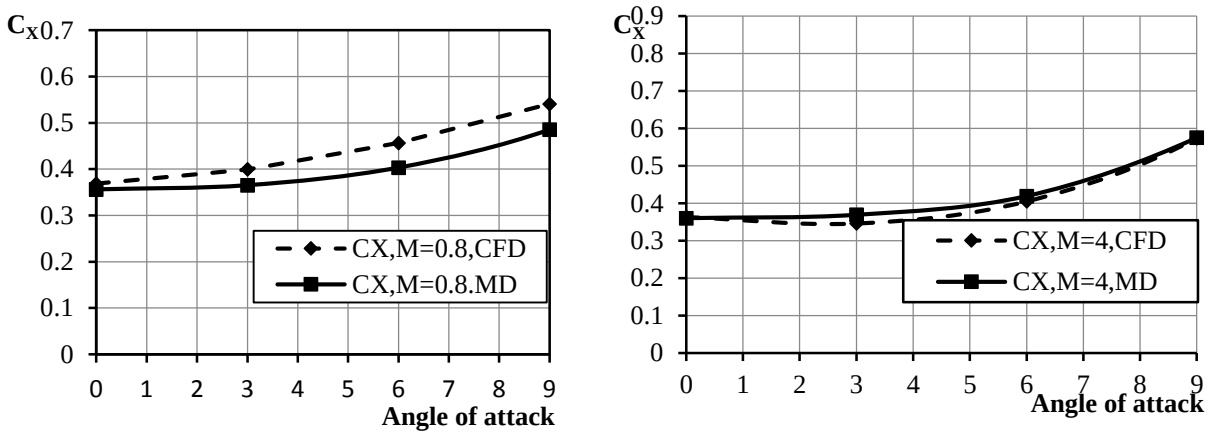

(a) (b)

Figure 4.1: The total drag force coefficient for various regions of speed

Figure 4.1.a shows the total drag force coefficient for missile's body in high subsonic region (M=0.8). The two solutions have the same tendency, but there is slight difference ranging approximately from 2 to 9 degree angle of attack between the Computational Fluid Dynamics method and the Missile Datcom method. This difference in results from the fact that, the Missile Datcom software calculates the coefficients based on the dimensions of the body that input to the software. These dimensions affected by boundary layer, so the CFD considered the boundary layer effect which means the diameter of the missile increased to be equal original diameter plus thickness of boundary layer which in turn have a strong impact on the base drag and thus affects the total value of the drag coefficient.

Figure 4.1.b represents the total drag force coefficient for missile's body in supersonic region (M=4). The two methods have the same tendency and the figure shows an satisfactory agreement between the CFD method and Missile Datcom method. In supersonic region the effect of boundary layer is very small because flow detaches the body due to shock wave appearance and then the wave drag is dominated.

Figure4.2.a,b shows the total lift force coefficient for missile's body for subsonic and supersonic regions.

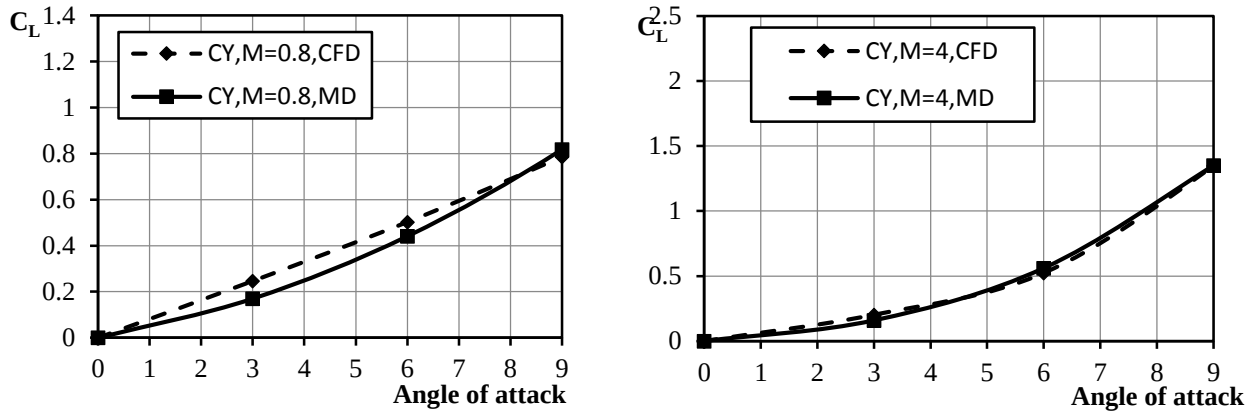

(a) (b)

Figure 4.2: The total lift force coefficient for various regions of speed

Figure 4.2.a shows the lift force coefficient for missile's body in subsonic region The same behavior is captured by the two software and there is a slight difference between the Computational Fluid Dynamic method and Missile Datcom method. The figure reveals that the lift coefficient increases with increase of angle of attack. Figure 4.2.b indicates the lift force coefficient for missile's body in supersonic region. The figure reveals very satisfactory agreement between the computational and analytical results.

Moreover the effect of the side wind considered as an important parameter in aerodynamics, therefore Figure 4.3 below shows the total side force coefficient for missile's body in subsonic and supersonic regions.

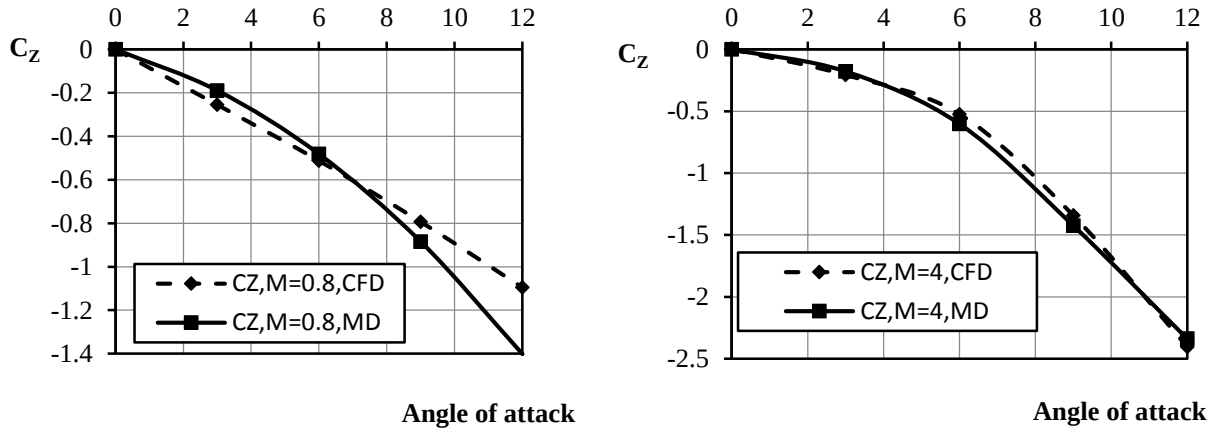

(a) (b)

Figure 4.2: The total lift force coefficient for various regions of speed

Figure 4.2.a represents the total side force coefficient for missile's body in subsonic region. The figure shows good agreement between the CFD and Missile Datcom methods.

Figure 4.3.b results the total side force coefficient for missile's body in supersonic regime. The figure shows very good satisfactory agreement between the computational technique and Missile Datcom program.

The previous results show an excellent agreement between the two techniques that have been used for supersonic region while slight divergence is observed for subsonic regime therefore, the Missile Datcom software can be considered as results validation tool indicating the accuracy of the computational fluid dynamics, CFD, approach.

4.3 Total configuration Results Analysis:

One of the main tasks is to investigate the phenomenon of the aerodynamics on the real missile geometry representing in this study by the second model that including the missile body with wrapped fins.

The effect of the wrapped fins interference with body on the aerodynamic coefficients is represented by the comparison illustrated in the table 4.1:

Table 4.1: Comparison of the aerodynamics characteristics effects on models

Parameters	Body	Body+Fins	Increment (absolute)
C_d	0.5409	0.6634	0.1224
C_l	0.7857	1.0681	0.2824
C_z	0	-0.1047	0.1047
C_{mz}	-2.2750	-6.3001	4.0251
C_{my}	0	1.2806	1.2806
C_{mx}	0	0.1611	0.1611

The table 4.1 compares the aerodynamics characteristics for the first model (Single body) with the second model (Body + wrapped fins) for Passive phase missile at angle of attack, AOA, = 9° and Mach number ,M, = 0.8.

Comparing with the single body, the corresponding lift coefficients for the body-fin combination has been improved significantly from 0.7857 to 1.0681. The lift coefficient, C_L, at $\alpha = 9°$ and $M = 0.8$ in particular has increased by about 35.942 per cent. It reveals that the aerodynamic interference and mutual coupling between the body and WAFs have actually enhanced the lift characteristics of the whole rocket. The WAFs have also made a high contribution to the longitudinal and lateral static stability of the whole rocket, e.g. the increment in the values of pitching moment coefficient in negative signs.

The corresponding pitching moment coefficient has been increased by about 176 percent, compared to the single body.

For the drag characteristics, the combined body and fin configuration is obviously enlarged the surface area of the entire rocket to a certain extent when introducing the WAFs and therefore the corresponding friction drag is increased.

As shown in Table 4.1, the corresponding drag has been increased by 22.63 per cent compared to the single body case at $\alpha = 9$ degree and $M = 0.8$.

4.3.1 Total configuration missile Active phase results (Motor on):

Missile Active phase or in some literature it is defined as Full Propellant Missile the case which represents the missile when the rocket motor produces thrust force due to combustion of the solid fuel, and in this case the condition of the back face of the rocket is defined in the preprocessing as mass flow rate.

The simulation for the model of the missile Active phase (Motor on) is performed and for the huge number of results and schematics beside the same flow behavior of the rest of the results, only a single scheme in subsonic flow regime with Mach number 0.4, single scheme in transonic flow regime with Mach number 0.9 and single scheme in supersonic flow regime with Mach number 2 is studied.

4.3.1.1 Drag force coefficient:

Figure 4.4(a, b and c) shows the total drag force coefficient for the missile at various regions of speed against range of angle of attack.

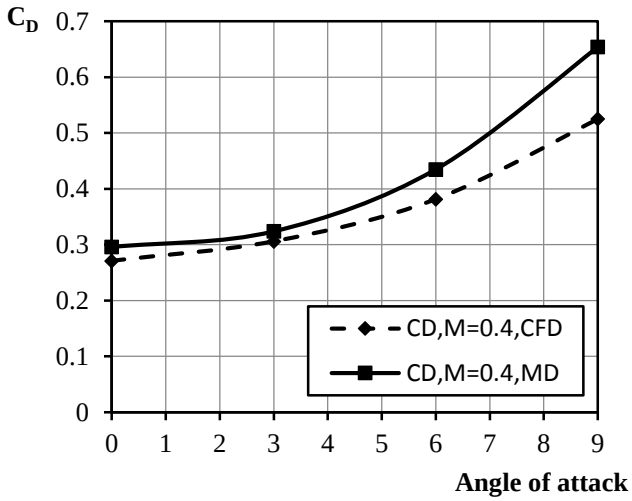

(a)

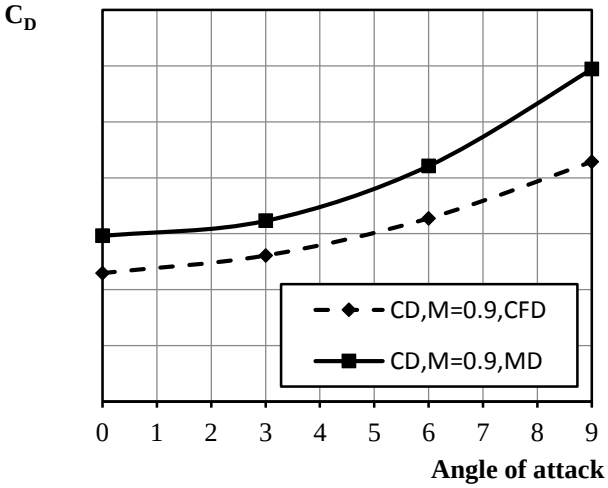

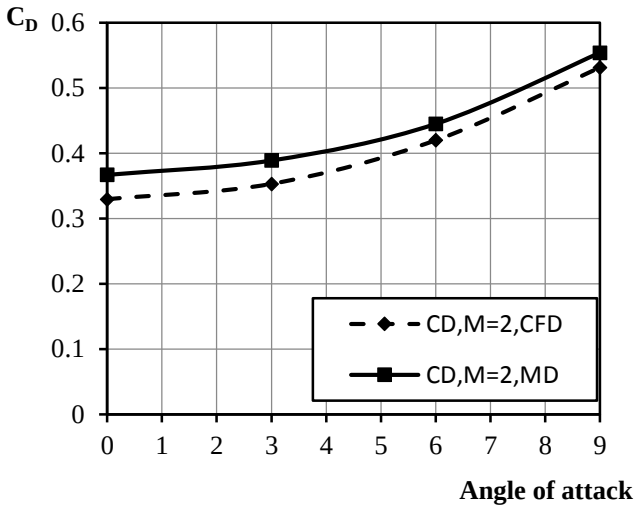

(b) (c)

Figure 4.4:the total drag coefficient for various regions of speed

Figure 4.4.a: indicates the total drag force coefficient for the missile in subsonic regime (M=0.4) versus range of angle of attack. From the Figure the two solutions provide the same tendency of the drag coefficient and there is slight difference in C_D between the CFD method and Missile Datcom method starts to increase regularly

after angle of attack 3 degrees. At angle of attack 9 degree the Drag coefficient reaches 0.17.

Figure 4.4.b: illustrates the total drag force coefficient for the missile in transonic flow regime (M=0.9) against range of angle of attack. According to the numerical software, the drag coefficient reads 0.3 at zero angle of attack. This value increases with angle of attack till 0.6 at 9 degrees.

The Figure 4.4.c also represents that the Computational Fluid Dynamics software is under-predicting the drag force by 0.067 at zero angle of attack, while at 9 degree angle of attack it is 0.166. It is observed from the result in Figure 4.4.c that both, software have the exact tendency till angle of attack 3 degree and then a slight divergence about 0.0855 is occurred gradually till angle of attack 9 degree.

Figure 4.4.c: shows the total drag force coefficient for the missile in supersonic flow regime (M = 2) against range of angle of attack.the increment in drag coefficient is occurred with increase of angle of attack. The drag coefficient at zero angle of attack is 0.3670 and 0.3295 read by Missile Datcom method and the CFD method respectively, whereas the coefficient at 9 degree is 0.5540 and 0.53142 indicated by Missile Datcom technique and the CFD technique respectively.

As shown in figure 4.4.a,band the value of drag coefficient computed by CFD has little delay from that computed by Missile Datcom this delay refers to:

- Missile Datcom uses free stream velocity at the missile's nose and fins entrance, but CFD uses corrected velocity due to the deceleration.
- Missile Datcom considered fins as planner, but CFD uses real shape of the fins.
- CFD considered boundary layer effect, but Missile Datcom does not consider the boundary layer effect.
- Also the effect of induced drag becomes dominated at high angle of attack .

The divergence between the two different calculation methods becomes small in supersonic flow region this convergence refers to the shape of shock wave is oblique in supersonic speed which has less strength compared with normal shock wave, and shock wave detaches flow which reduces the effect of boundary layer.

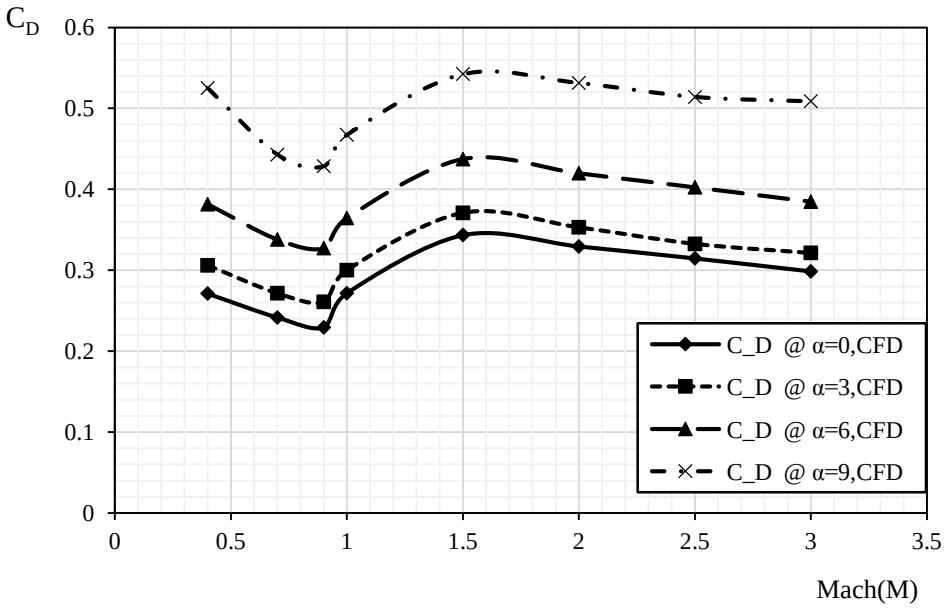

Figure 4.5: The total drag coefficient against velocity

Figure 4.5: shows the total drag force coefficient for the whole regions of speed and angle of attack. It is obvious that the total Drag coefficient is increase with increase of angle of attack .The total Drag coefficient starts to decrease with the increase of speed because the friction drag has strong effect on the body at low speed while this effect is reduces with increase of speed.

With continuous increase in speed till reach the transonic regime and approximately at M = 0.9, the C_D starts to increase sharply due to the effect of normal shock wave which has the maximum wave drag. This increment in drag coefficient continuous until M = 1.6 and then with the increase of speed the Drag coefficient starts again to decrease slightly as shown in Figure 4.5.

The decrease in total Drag at supersonic speed is a result of the shape of shock wave which becomes oblique in supersonic speed with less strength compared with normal shock wave that occurs at transonic speed. Moreover, at supersonic regime the oblique shock wave detaches the flow from the boundary layer which leads to reduction in skin friction drag and therefore reduction in the total drag coefficient at supersonic flow regime with the increase of Mach number.

It is clear that the Drag coefficient is very sensitive to the angle of attack since highest values of drag are captured by the CFD and Missile Datcom programs.

The effect of speed (Mach number) from subsonic to supersonic regions on the Drag coefficient is less compared with airfoil profile that representing some dramatic phenomena.

It is obvious in subsonic and supersonic regions, the Missile Datcom program is representing high Drag coefficient than CFD results due to consideration of the wrapped fins as a planner fins in Missile Datcom inputs.

4.4.1.2 Lift force coefficient:

The lift coefficient is strongly affected by the fin parameters such as fins span, fins chord, thickness, leading-edge sweep, curvature radius, fin numbers, setting angles and airfoil section.

Figure 4.6(a, b and c): illustrates the total lift force coefficient for various regions of speed.

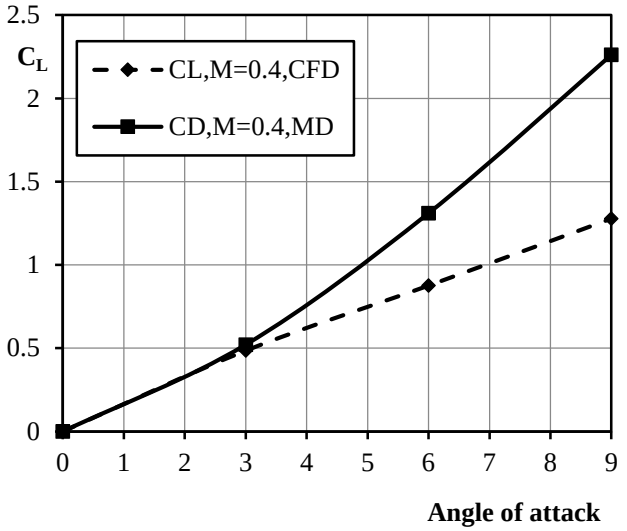

(a)

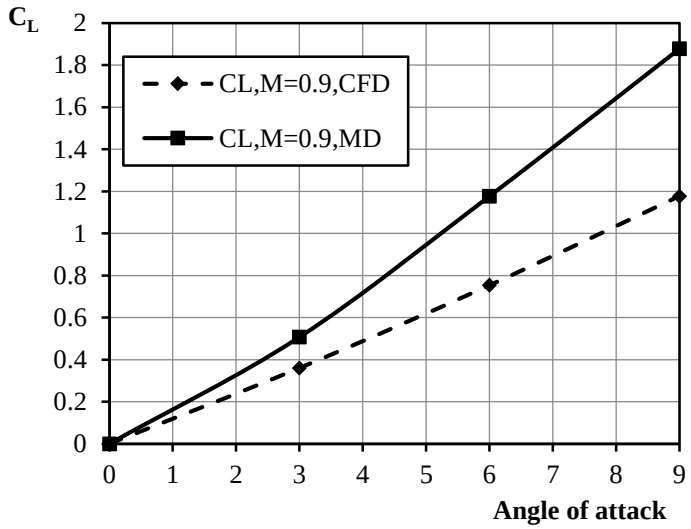

(b)

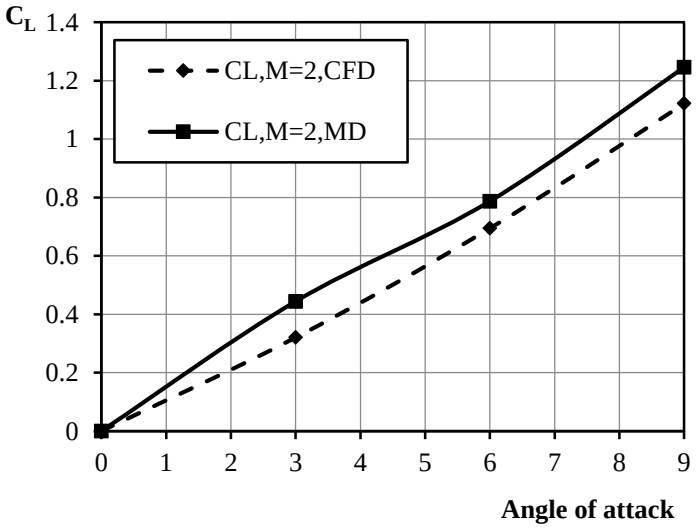

(c)

Figure 4.6: The total lift force coefficient for various regions of speed

Figure 4.6.a shows the total lift force coefficient for the missile in subsonic flow region at M=0. versus angle of attack.The lift coefficient predicted by Missile Datcom program increases gradually till angle of attack 3 degrees where it is approximately 0.5 then increases sharply with high slop to 2.261 at 9 degrees angle of attack.

The lift coefficient that numerically calculated is reveals full agreement with analytical result till 3 degree after that a large divergence is observed. The numerical program keeps the same slop till 9 degrees angle of attack where the lift coefficient is 1.2777. The difference in reading between CFD method and Missile Datcom method refers to fins shape. The CFD deals with real fins shape (wrapped around fins) whereas the Missile Datcom deals with fins as planner fins.

Figure 4.6.b illustrates the total lift force coefficient for the missile in transonic flow region at M=0.9 versus angle of attack.

With increase of speed to transonic, the divergence between the two programs starts too early at angle of attack 0.4 or less. This divergence increases largely after 3 degrees angle of attack. The slope of Missile Datcom program is higher than the slope of Computational Fluid Dynamics program to captures lift coefficient 1.878 at 9 degrees angle of attack whereas the CFD reads 1.177 at the same angle.

Figure 4.6.c represents the total lift force coefficient for the missile in supersonic flow region at Mach number 2 against angle of attack.The figure provides an exact tendency between two programs with constant under-predicting of CFD till angle of attack 9 degrees.

The lift coefficient indicated by Missile Datcom and computational technique at 9 degrees is 1.246 and 1.1219 respectively. No delay, but constant divergence is captured between the two programs in supersonic regime up to 0.1241.

As stated before, the delay in under-predicting of numerical solution for the lift coefficient at higher angle of attack results from the fact that the planner fins defined for Missile Datcom program is generate more lift than the real wrapped around fins introduced to numerical program ,and free stream was used in Missile Datcom program.

4.3.1.3 Side force coefficient:

It is well known that the single body is a critical symmetric geometry, which cannot generate the side force effectively. However, due to the presence of the wrapped around fins (WAF), the whole rocket has generated the extra side force and side moment. Because of the effect of the angle of attack, the pressure on the lower fins becomes higher than that of the upper fins. These elements result in an unbalance in the pressure distribution, and generate the side forces which are perpendicular to the plane of the free stream.

Figure 4.7(a,b and c): illustrates The total side force coefficient for various regions of speed.

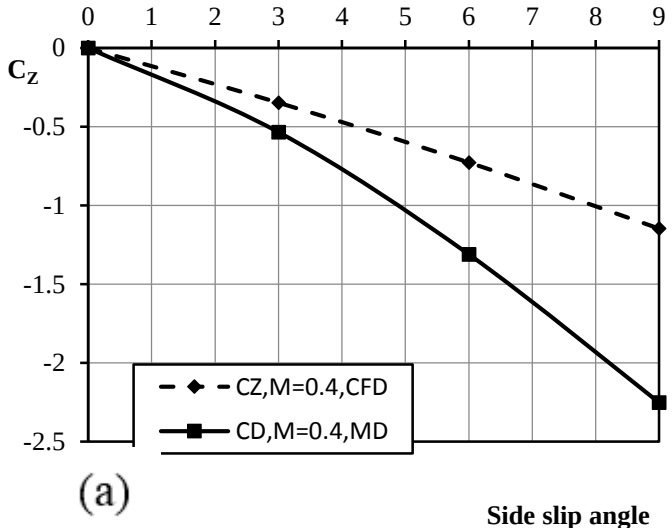

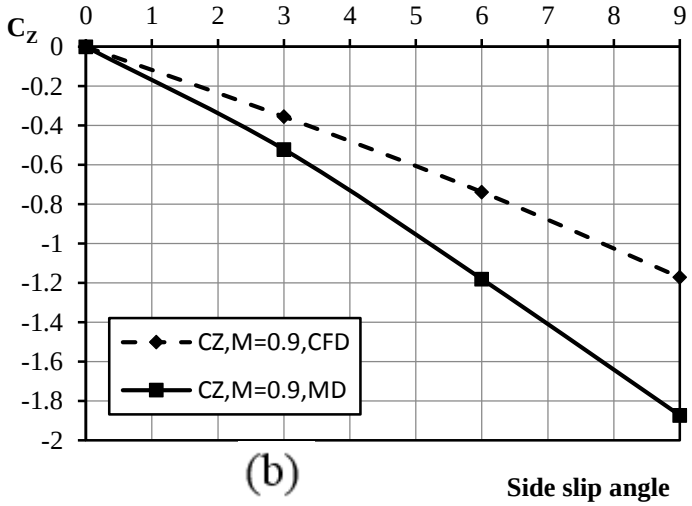

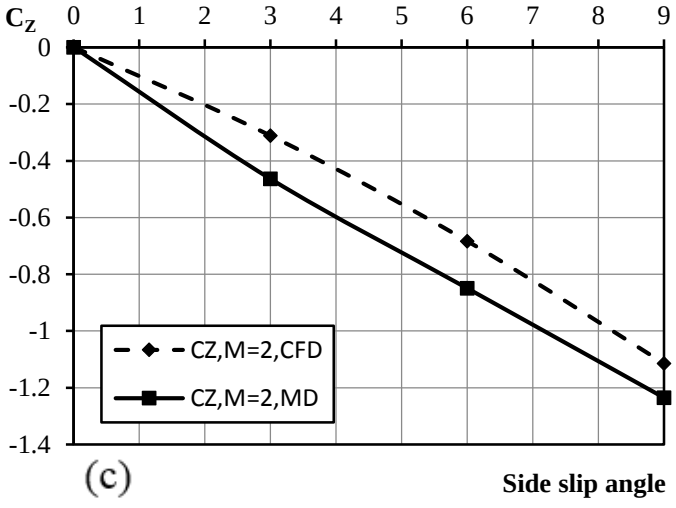

Figure 4.7: The total side force coefficient for various regions of speed

Figure 4.7.a determines the total side force coefficient for whole missile in subsonic flow region at Mach number 0.4 versus angle of attack.

Missile Datcom program predicts -2.252 Side Force coefficient at 9 degree angle of attack whereas only -1.1467 is predicted by CFD at the same angle.

The Missile Datcom program represents large change in Side Force coefficient along the change of angle of attack compared with the Computational Fluid Dynamic in subsonic region.

Figure 4.7.b shows the total side force coefficient for the missile in transonic flow region at Mach number 0.9 versus angle of attack. The same behavior at subsonic region for the Missile Datcom and Computational program is observed at transonic region with less divergence.

The side force coefficient indicated by the MD is -1.872 at 9 degree angle of attack whereas the CFD calculates -1.1707 at the same angle of attack.

The variation in reading between the programs is decreased with increment in speed.

Figure 4.7.c illustrates the side force coefficient for the missile in supersonic flow region at Mach number 2 versus angle of attack.

The divergence between the codes is reduced to 0.1207 at 9 degree angle of attack with increase the speed to supersonic speed. The side force coefficient is -1.235 and -1.1143 at 9 degree angle of attack predicted by MD and CFD respectively.

The two methods have same tendency and slop from approximately 3 degree angle of attack to 9 degree. The over-predicting of CFD is clearly reduced in supersonics speed.

4.4.1.4 stability characteristics:

The missile has four fins of a cruciform configuration. The cross section of the fins along the chord is a symmetric airfoil. Fins in open condition are providing stability and control of the missile at all time of the flight mission.

The aerodynamic moments are create rotation around the longitudinal body axes and angular motion around the Y and Z body axes, combined around the center of gravity.

The corresponding aerodynamic coefficients are C_{mx} ,C_{my} ,$C_{mz}$for rolling, yawing and pitching moments respectively.Each angular motion induced corresponding damping moments and aerodynamic damping moment coefficients.

For the stability coefficients prediction, the CFD technique only is considered because it is deal with exact model of the Missile.

4.4.1.4.1 Pitching moment coefficient (C_{mz}):

Winged device undergoes lift during flight. In common cases, the lift will produce longitudinal moment, namely pitch moment**.** The pitching moment coefficient **(C_{mz})** defines longitudinal static stability coefficient or Stability margin. During motor on phase of flight, the center of gravity position $Xc.g.$ is changeable due to fuel combustion during the flight task and the effect of flight Mach number.

Figure 4.8(a,b and c) represents the pitching moment coefficient for the missile in several flow regions versus angle of attack.

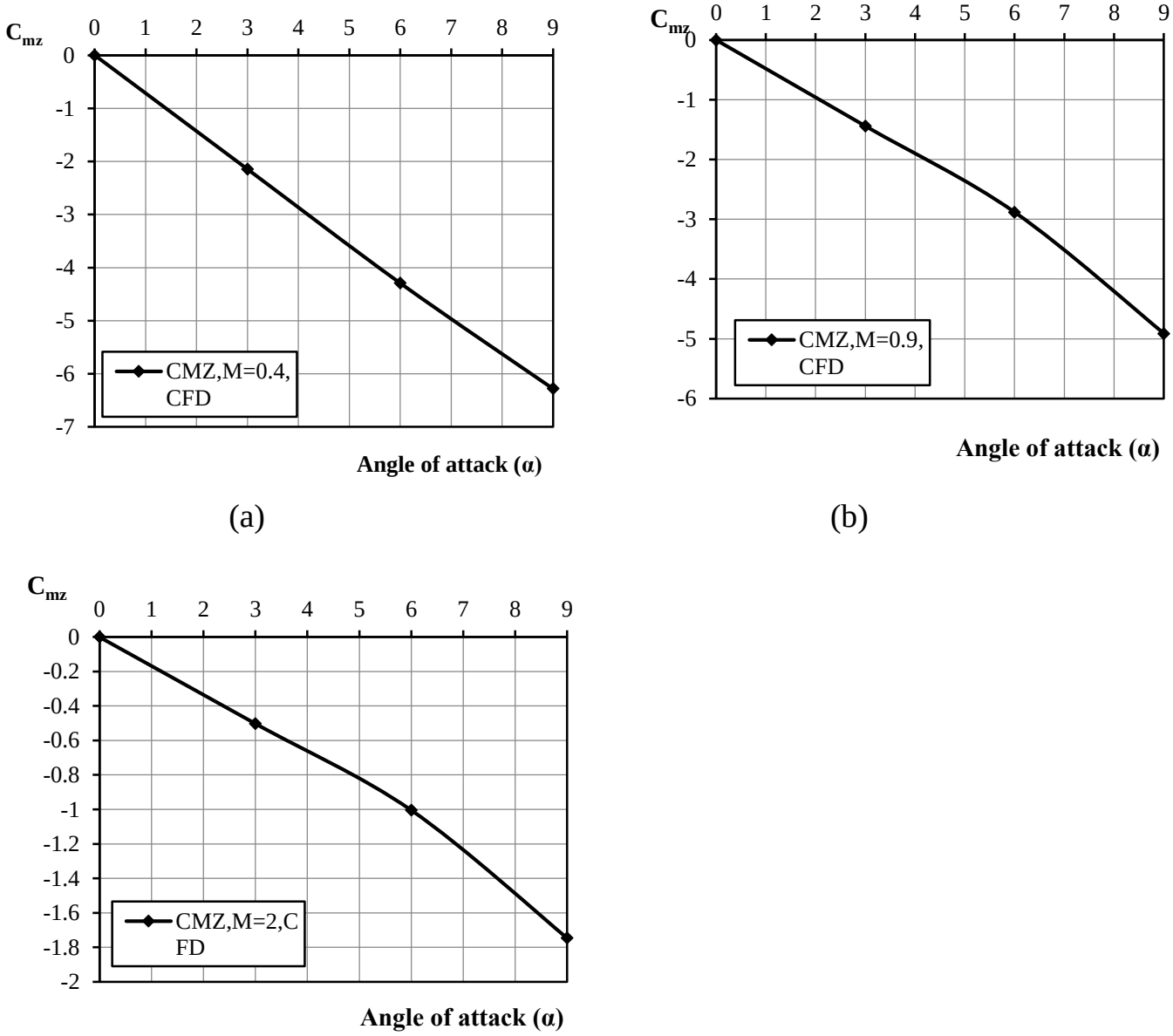

Figure 4.8: The pitching moment coefficient for different speed regions

The Figure 4.8.a represents a negative slope for C_{mz} versus angle of attack which indicates the stability of the flaying object and means that the center of pressure is located after the center of gravity, so the missile is longitudinally stable. The slope of the coefficient is -0.6978 and the pitching moment coefficient is -6.2804 at 9 degree of attack.

Figure 4.8.b shows the pitching moment coefficient for the missile in transonic flow region at Mach number 0.9 against angle of attack.

The Figure represents the stability of the Missile at transonic region. The negative slope is 0.4802 till angle of attack 6 degree where the pitching moment coefficient is -2.8812 then it is change to 0.67673 which is closed to subsonic region for 7, 8 and 9 angles of attack. The pitching moment coefficient is -4.9114 at 9 degree angle of attack.

Figure 4.8.c shows the pitching moment coefficient for the missile in supersonic flow region at Mach number 2 versus angle of attack.

The behavior of pitching moment coefficient at supersonic region is similar to that at transonic region with different in slopes.

The negative slope in supersonic region is decreased compared with transonic speed. The slope is -0.167395 till 6 degree and then switches to -0.247377 at 9 degree angle of attack.

The pitching moment coefficient is -1.00437 and -1.7465 at 6 and 9 degree angle of attack respectively and the negative value of slope indicates the stability of the missile in supersonic region too.

4.4.1.4.1 Yawing moment coefficient (C_{my}):

Since the stability of the entire rocket is affected by the additional side forces generated by WAF, the yawing moment coefficient **(C_{my})** defines lateral static stability coefficient and depends on flight Mach number.

Figure 4.9. represents the yawing moment coefficient for the missile in range of speed regions versus side slip angle.

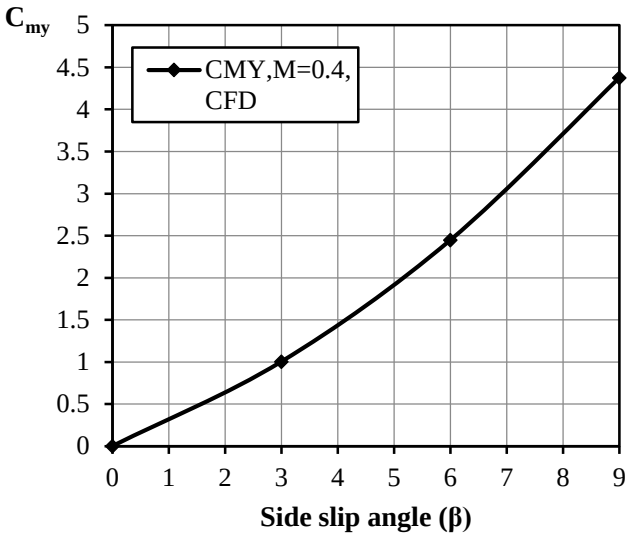

(a)

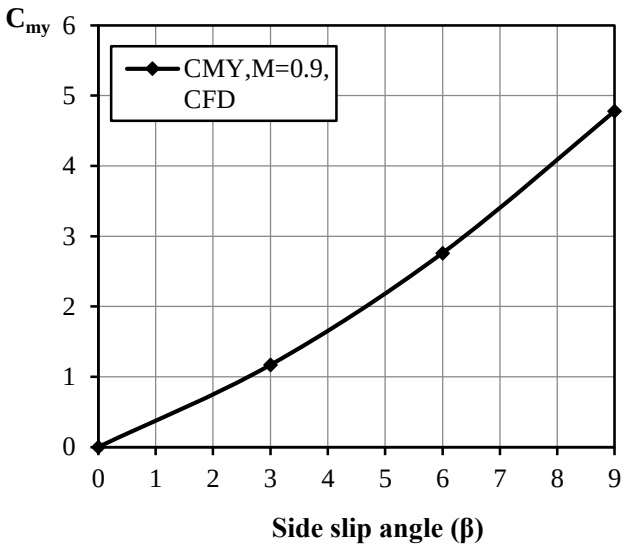

(b)

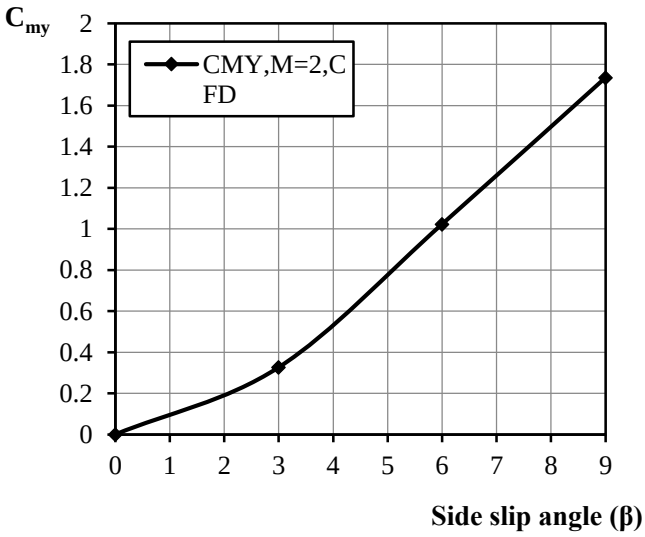

(c)

Figure 4.9 The yawing moment coefficient for different speed regions

The Figure 4.9.a: above represents positive slop which indicates the stability of the missile in lateral direction. The yawing coefficient in subsonic (M=0.4) region is increases gradually till 4.376 at 9 degree angle of attack.

Figure 4.9.b shows the yawing moment coefficient for the missile in transonic flow region (M=0.9) against range of side slip angle.

The yawing moment coefficient is increases slightly with increase in speed. It reaches 4.779 at 9 degree angle of attack. The stability of the missile in lateral direction is ensured since the Figure represents positive slope.

Figure 4.8.c indicates the yawing moment coefficient for the missile in supersonic flow region at Mach number 2 versus side slip angle.

The figure indicates that the missile is stable in lateral direction in all flight speed regions subsonic, transonic and supersonic.

The positive yawing moment coefficient is increases gradually up to 0.3264 at 3 degree side slip angle then a large divergence in slope is occur till angle of side slip 9 degree where the coefficient is 1.7356.

It is clear that the yawing moment coefficient is decreases sharply with speed increment from 4.779 at transonic region to 1.7356 at supersonic region. The positive slope in the range from zero to 3 degree side slip angle is 0.1088 whereas at the rest of angles it is 0.23486.

4.3.2 Total configuration missile Passive phase results (Motor off):

Missile Passive phase or in some literature it defined as Empty Propellant Missile the case which illustrates the results of simulation when the rocket motor doesn't produce thrust force (passive phase) and the missile depends only on the inertia force, and in this case the condition of the back face of the missile is defined as wall and the base drag is generated at the back face.

The simulation for the model of themissile Passive phase (Motor off) is performed and for the huge number of results and schematics beside the same flow behavior of the rest of the results, only a single scheme in subsonic flow region with Mach number 0.4, single scheme in transonic flow region with Mach number 0.9 and single scheme in supersonic flow region with Mach number 2.5 will discuss in this section.

4.4.2.1 Drag force coefficient:

Figure 4.9 (a ,b and c)represents the total drag force coefficient for whole missile at subsonic ,transonic and supersonic flow regions against range of angle of attack.

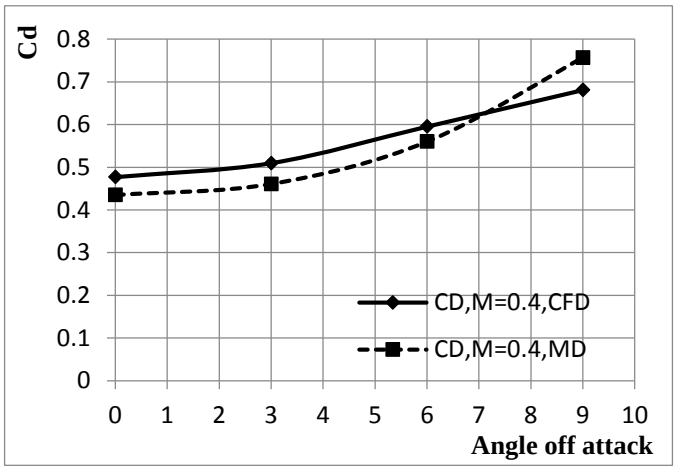

(a)

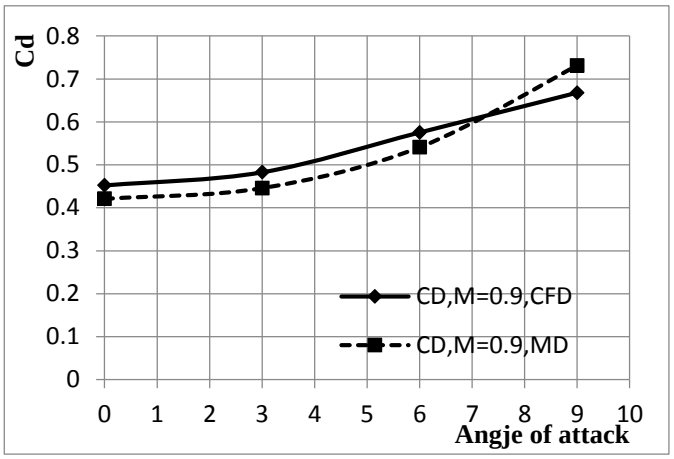

(b)

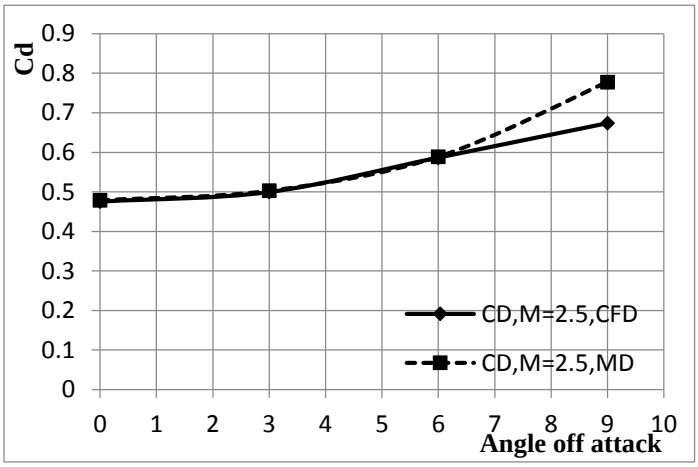

(c)

Figure 4.9: the total drag force coefficient for various speed regions

Figure 4.9.a: reveals the total drag force coefficient for the Missile in subsonic flow region (M=0.4) versus angle of attack. The increment in drag coefficient is occurred with increase of angle of attack .The two programs represent a very good satisfactory agreement from zero angle of attack till 6 degree. and after that the slop of Missile Datcom increases more than CFD slop.

The numerical program is over-predicting the drag coefficient by only 0.0418 at zero angle of attack increased gradually to 0.03235 at 6degree,at angle of attack 9 degree Missile Datcom reaches 0.7615 over CFD value .

Figure 4.9.b:shows the total drag force coefficient for the Missile in transonic flow region (M=0.9) against range of angle of attack. drag coefficient proportions with angle of attack The drag coefficient at zero angle of attack is 0.421 and 0.45217 read by Missile Datcom method and the CFD method respectively, whereas the coefficient at 9 degree is 0.731 and 0.668 indicated by Missile Datcom technique and the CFD technique respectively.

At Mach number 0.9 the Missile Datcom results under-predicting of drag coefficient for angle of attack from zero to 7 degree but at high angle of attack Missile Datcom results over-predicting of drag coefficient. the slight difference between the results of the programs is because of thebase drag which is strongly affected by the boundary layer.

Figure 4.9.c: illustrates the total drag force coefficient for the Missile in supersonic flow region (M=2.5) through a range of angle of attack. the two solutions have the same propagation and the flow behavior. It is observed that till angle of attack 6 degree two methods are close to each other and with increase of angle of attack above 6 degree the Missile Datcom method has a little bit diverges regularly after angle of attack 6 degree from the computational method till angle of attack 9 degree where the difference in Drag coefficient is 0.104. The drag force represented by both programs increases gradually from zero angle of attack till 6degree angle of attack and then sudden sharp increases till 9degree angle of attack.

It seems that in subsonic and transonic regions, the Computational Fluid Dynamics technique [CFD] has a little delay in over-predicting the drag coefficient till 7degree

angle of attack. This over-prediction due boundary layer which has strong effect on the dimensions specially base diameter which generates base drag .

It is obvious in subsonic and transonic regions, the CFD program is representing high Drag coefficient than Missile Datcom results due to boundary layer effect.

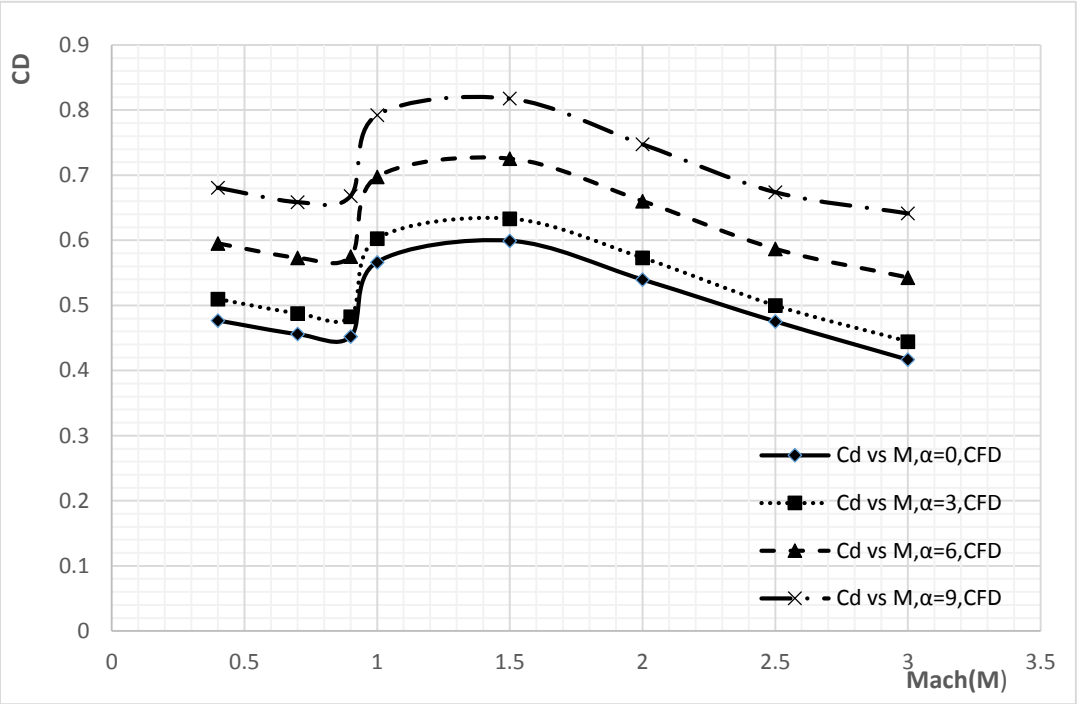

Figure 4.10. The total drag coefficient against Mach

Figure 4.10: shows the total drag force coefficient for whole regions of speed and angle of attack. It is obvious that the total Drag coefficient increases with increase of angle of attack .The total Drag coefficient starts to decrease with the increase of because at low speed the friction drag has strong effect and reduces with increase of speed and with continuous increase in speed till reach to transonic region from M=0.9 CD starts to increase sharply due to effect of normal shock wave which has maximum wave drag and this increment in drag coefficient continuous until reaches M=1.5,and then with the increase of speed the Drag coefficient starts to decrease slightly as shown in figure this decrease in supersonic speed as a result of the shape

of shock wave becomes oblique in supersonic speed which has less strength compared with normal shock wave which occurs in transonic speed ,also in supersonic regime the oblique shock wave detaches flow from the boundary layer which leads to decrease the skin friction drag ,then the total drag coefficient decreases in supersonic flow region with the increase of Mach number .

It is clear that the Drag coefficient is very sensitive to the angle of attack since highest values of drag are captured by the CFD and Missile Datcom programs.

The effect of speed (Mach number) from subsonic to supersonic regions on the Drag coefficient is less compared with airfoil profile that representing a dramatic phenomenon.

4.4.2.2 Lift force coefficient:

the lift coefficient is strongly affected by the wing parameters such as fins span, fins chord , thickness, leading-edge sweep, curvature radius, fin numbers, setting angles and airfoil section.

Figure 4.5(a,b and c)) shows the total lift force coefficient for whole missile in subsonic(M=0.4), transonic(M=0.9) and supersonic flow region (M=2.5)against range of angle of attack .

From the figures below the two methods graphs behave like each other and the lift coefficient increases with increase of angle of attack ,and there is difference between **CFD** method and Missile Datcom method and this difference refers to fins shape ,CFD deals with real fins shape (wrapped around fins) but Missile Datcom deals with fins as planner fins so lift force generated by flat fin is much compared with wrapped fins .

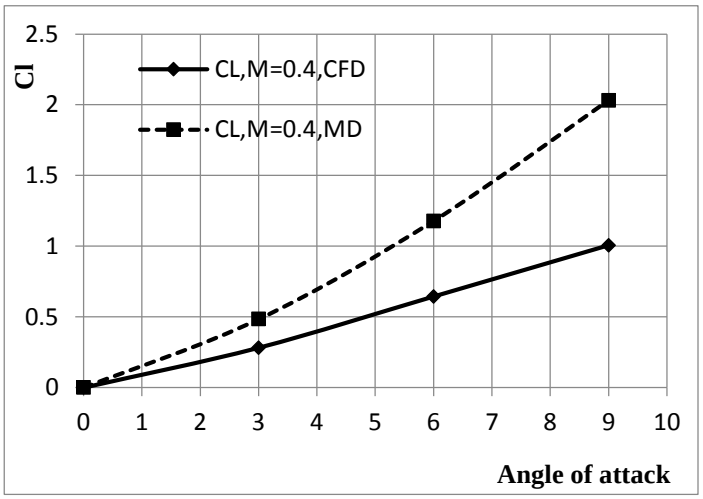

(a)

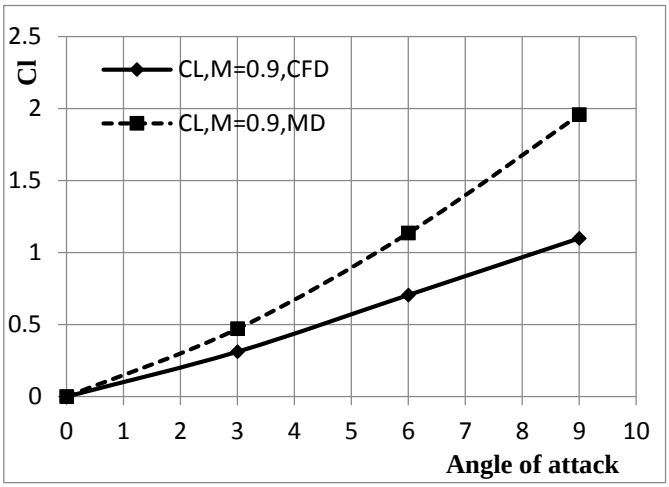

(b)

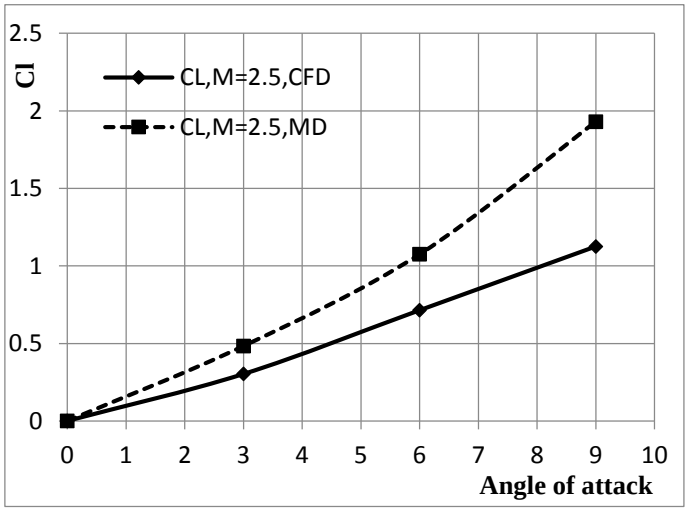

(c)

Figure 4.11: The total lift force coefficient for various regions of speed

Figure 4.11.a shows the total lift force coefficient for the missile in subsonic flow regions at Mach number 0.4 versus angle of attack.The lift coefficient predicted by Missile Datcom program increases gradually till angle of attack 3 degrees where it is 0.48 then increases sharply with high slop to 2.03 at 9 degrees angle of attack.

The lift coefficient that numerically calculated is reveals same behavior ofanalytical result,the divergence between the two programs starts too early. This divergence increases largely after 3 degrees angle of attack. The slope of Missile Datcom program is higher than the slope of Computational Fluid Dynamics program to captures lift coefficient 2.03 at 9degrees angle of attack whereas the CFD reads 1.005 at the same angle.

The numerical program keeps approximately the same slop till 9degrees angle of attack where the lift coefficient is 1.005. The difference in reading between CFD method and Missile Datcom method refers to fins shape. The CFD deals with real fins shape (wrapped around fins) whereas the Missile Datcom deals with fins as planner fins.

Figure 4.11.b illustrates the total lift force coefficient for the missile in transonic flow regions with Mach number 0.9 versus angle of attack. With increase of speed to transonic speed, the divergence between the two programs starts too early at angle of attack 0.4 or less. This divergence increases largely after 3degree angle of attack. The slope of Missile Datcom program is higher than the slope of Computational Fluid Dynamics program to captures lift coefficient 1.957 at 9degree angle of attack whereas the CFD reads 1.09 at the same angle.

As stated before, the delay in under-predicting of numerical solution for the lift coefficient at higher angle of attack results from the fact that the planner fins defined for Missile Datcom program is generate more lift than the real wrapped around fins introduced to numerical program ,and free stream was used in Missile Datcom program

Figure 4.5.c represents the total lift force coefficient for the missile in supersonic flow region at Mach number 2.5 against angle of attack.

The figure provides an exact tendency between two programs with constant under-predicting of CFD till angle of attack 9 degrees.

The lift coefficient indicated by Missile Datcom and computational technique at 9 degrees is 1.93 and 1.12 respectively. No delay, the divergence becomes small till angle of attack 6 degree and increases at angle of attack 9 degree captured 0.81.

4.4.2.3 Side force coefficient:

It is well known that the single body is a critical symmetric geometry, which cannot generate the side force effectively. However, due to the presence of the wrapped around fins (WAF), the whole rocket has generated the extra side force and side moment. Due to the effect of the angle of attack of, the pressure on the lower fins becomes higher than that of the upper fins . All these elements can result in an unbalance in the pressure distribution, and generate the side forces which are perpendicular to the plane of the free stream.

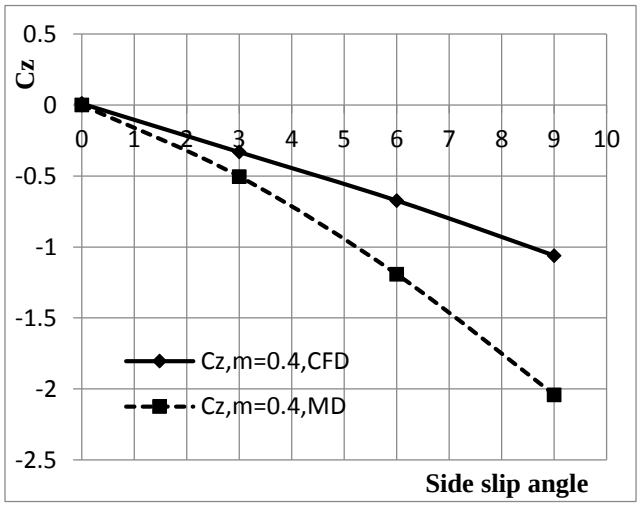

(a)

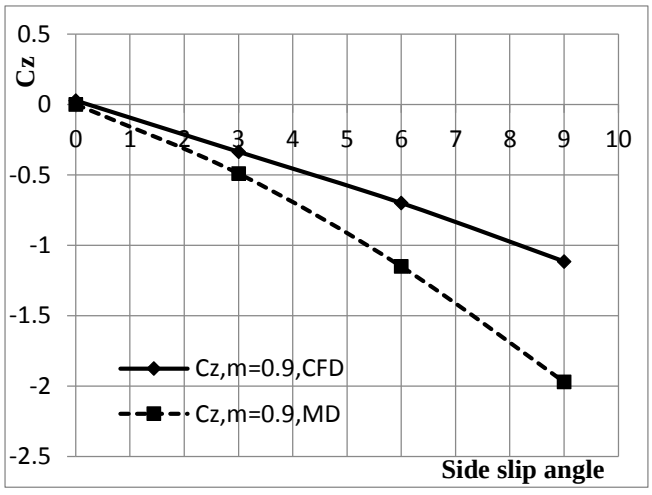

(b)

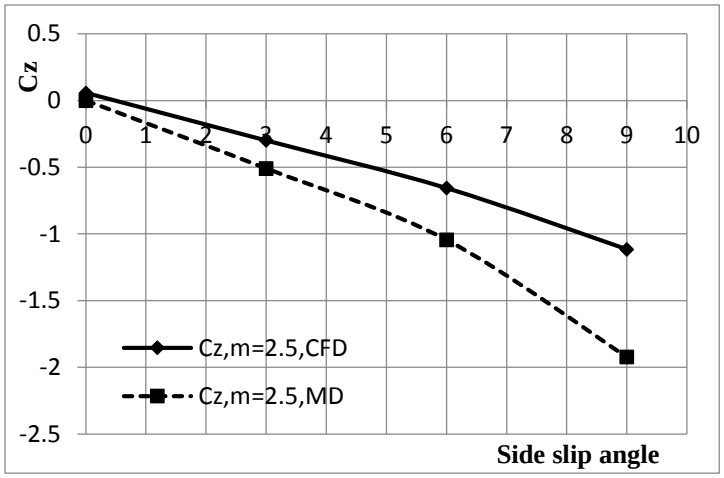

(c)

Figure 4.12 the total side force coefficient for various speed regions

Figure 4.12.a illustrates the total lift force coefficient for the missile in subsonic flow regions with Mach number 0.4 versus angle of attack. With increase of angle of attack, the divergence between the two programs starts too early at angle of attack . This divergence increases largely after 3degrees angle of attack. The slope of Missile Datcom program is higher than the slope of Computational Fluid Dynamics program in negative direction to captures side force coefficient -2.041 at 9degree angle of attack whereas the CFD reads -1.0607 at the same angle.

Figure 4.12.b shows the total side force coefficient for the missile in transonic flow region at Mach number 0.9 versus angle of attack.

The same behavior at subsonic region for the Missile Datcom and Computational program is observed at transonic region with less divergence.

The side force coefficient indicated by the MD is -1.972 at 9 degree angle of attack whereas the CFD calculates -1.1156 at the same angle of attack.

The variation in reading between the programs is decreased with increment in speed.

Figure 4.12.c: shows the total side force coefficient for the missile at M = 2.5 against range of angle of attack.

The increment in side force coefficient is occurred with increase of angle of attack (in negative direction) ,At Mach number 2.5 the CFD results under-predicting of drag coefficient. This under-prediction is increased to be 0.8 at 9 degree angle of attack.

As analyzed previously that slight difference between the results of the programs is because of fins shape considered in Missile Datcom program

4.4.2.4 stability characterestics:

The missile has four fins of a cruciform configuration. The cross section of a fins along the chord is an symmetric airfoil. fins in open position provide stability and control of a missile, all time of flight.

The aerodynamic moments created rotation around the longitudinal body axes and angular movement around Y and Z body axes, combined around the center of gravity. Corresponding aerodynamic coefficients are C_{mx} ,C_{my} ,$C_{mz}$for rolling, yawing and pitching moments. Every angular movement induced corresponding damping moments and aerodynamic damping moment coefficients.

For the stability coefficients the CFD method only was used because CFD method deals with real geometry .The moment coefficient is a much aerodynamic characteristics affected by weight reduction due to fuel combustion , so the center of gravity is changed in empty propellant case and moved forward .

4.4.2.4.1 pitching moment coefficient (C_{mz}):

Winged device undergoes lift during flight. In common cases, the lift will produce longitudinal moment, namely pitch moment**.** The pitching moment coefficient **(C_{mz})** defines longitudinal static stability coefficient or Stability margin. During motor off phase of flight, the center of gravity position $Xc.g.$ is not changeable.

Figure 4.13: (a,b and c) shows the pitching moment coefficient for whole missile in subsonic, transonic and supersonic flow region against range of angle of attack .

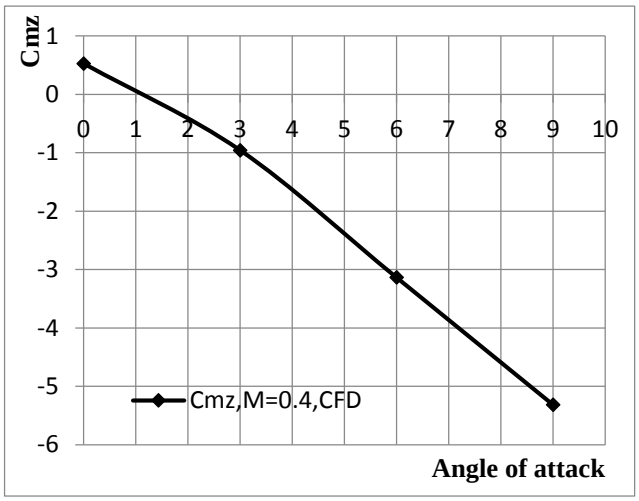

(a)

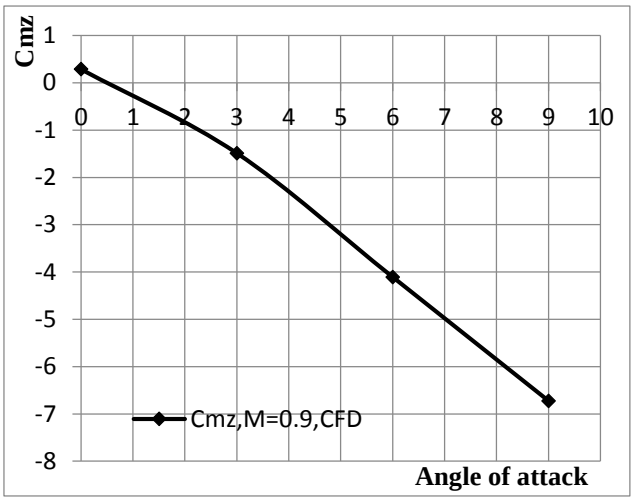

(b)

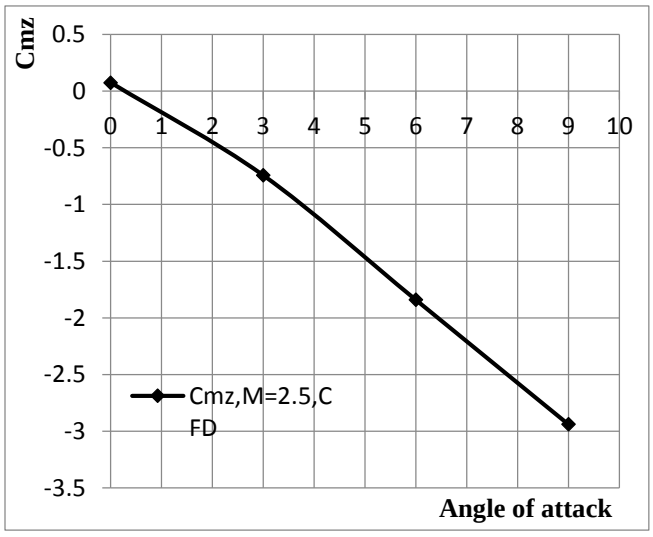

(c)

Figure 4.13 the pitching moment coefficient for various regions of speed

Figure (4.13.a) reviles the pitching moment coefficient for whole missile in transonic flow region (M=0.4) against range of angle of attack From figure the pitching moment increases gradually with angle of attack ,the computational technique reads -5.31 at 9degree and results slop is -1.511 which indicates to the stability of the missile and this means that the center of pressure locates after of the center of gravity, so the missile is longitudinally stable. pitching moment coefficient is strongly affected by lift force.

Figure (4.13.b) shows the pitching moment coefficient for whole missile in transonic flow region (M=0.9) against range of angle of attack. the figure indicates that the missile is stable in transonic region and the slop captured -1.25 the slope is less somehow compared with subsonic region this refers to the shock wave effects in transonic zone and the nature of the flow complicated at this region of speed.

Figure (4.13.c) illustrates compute pitching moment coefficient for the missile in supersonic flow region (M=2.5) versus angle of attack. the figure explains how does pitching moment increase with the increase of angle of attack and graph slop reaches -2.94. in the same manner increase of speed till supersonic speed provides more longitudinal stability .

4.4.2.4.1 yawing moment coefficient (C_{my}):

Because the stability of the entire rocket can be affected by the additional side forces generated by WAFs.The yawing moment coefficient **(C_{my})** defines lateral static stability coefficient and depends on flight Mach number and side slip angle.

Figure 4.14.(a,b and c) shows the yawing moment coefficient for whole missile in various speed regions against range of side slip angle of .

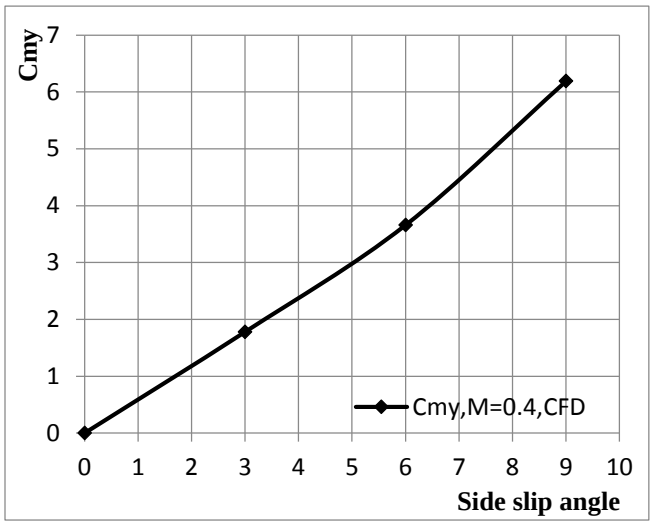

(a)

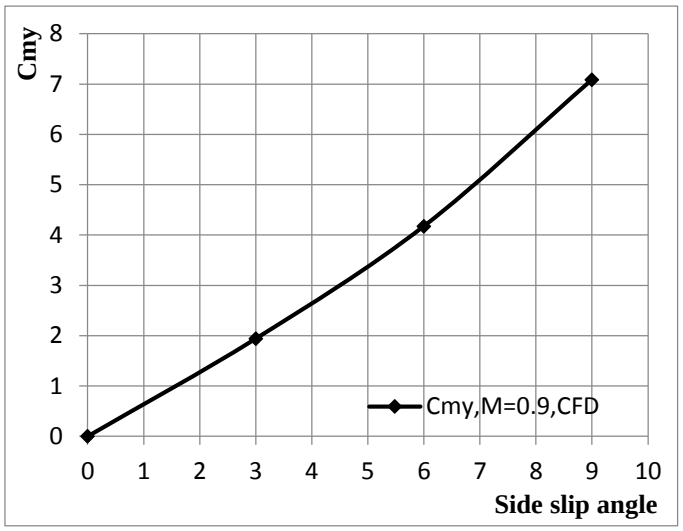

(b)

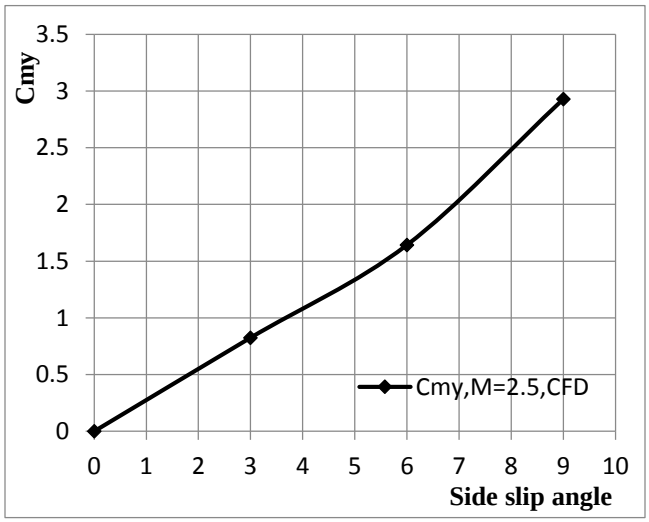

(c)

Figure 4.14 the yawing moment coefficient for various regions of speed

Figure 4.14.a shows thepitching moment coefficient for whole missile in subsonic flow region (M=0.4) against range of side slip angle ,obviously the graph has positive slop which indicates to the stability of flaying object in lateral direction the method reads slop as 1.4 at this speed region.

Figure 4.14.b provides a results of pitching moment coefficient for whole missile in transonic flow region (M=0.9) this region of speed represent the region of shock

wave and flow variation so the slop of the result decreased compared with previous flow region to reach 1.26 and missile still stable.

Figure 4.14.c represents the pitching moment coefficient for whole missile in supersonic flow region (M=2.5) it is touchable that the yawing moment increases with the increase of side slip angle and speed so the slop reaches 3.08.

As mentioned above missile is stable in lateral direction .

4.4.3 rolling moment coefficient (C_{mx}): :

The generation mechanism of the self-induced rolling momentComparing with the flat fin, the most important feature for the WAF is the self-induced rolling moment and its reversion under different flight conditions. When the air flows over the WAF the rolling moment from the convex to concave surfaces of WAF will be generated in subsonic flight, while during the supersonic flight condition, the rolling moment will be reversed. This reversion always happens near M =1 as a results of the shock wave. It may also reverse repeatedly in the supersonic range.

Figure 4.16 below shows the roll moment coefficient for different speed regions.

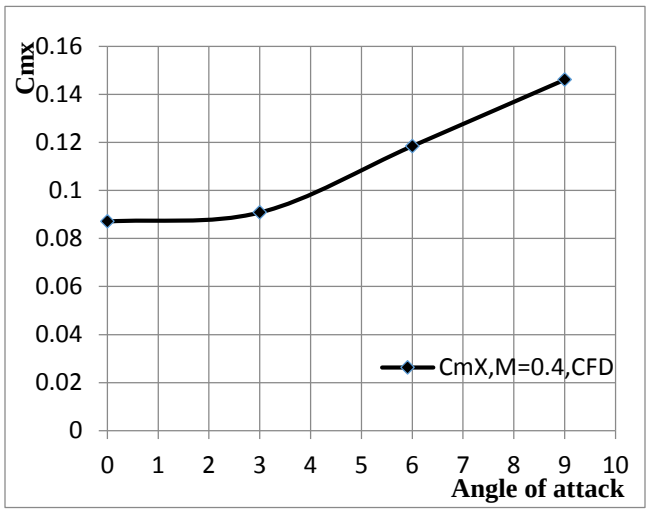

(a)

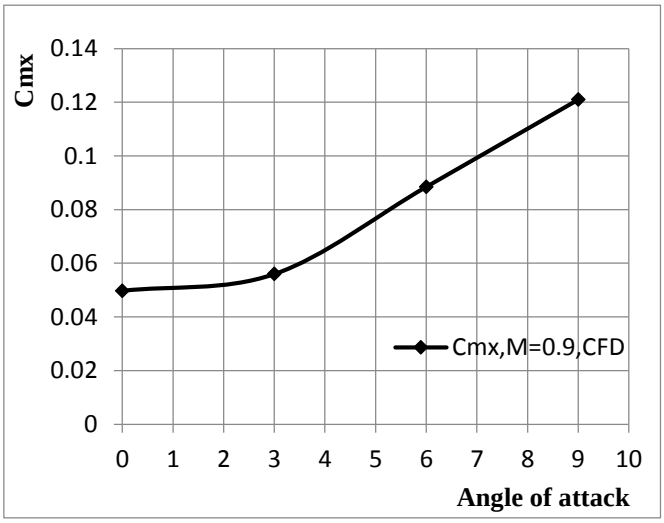

(b)

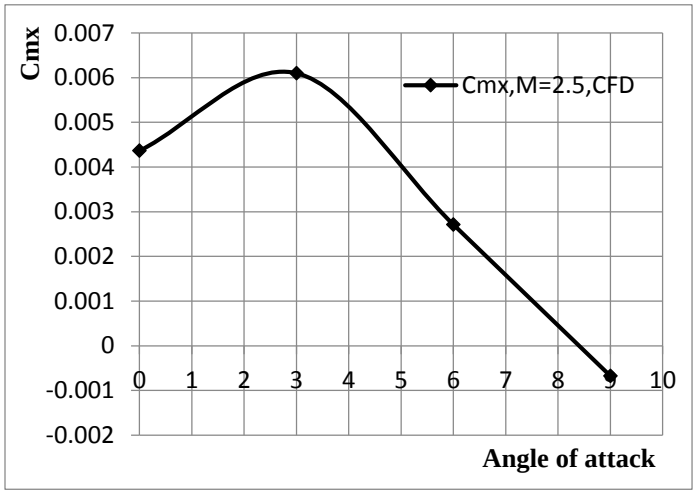

(c)

Figure4.16: Roll moment coefficient for various regions of speed

Figure 4.16.a: represents the pitching moment coefficient for whole missile in subsonic flow region (M=0.4) against range of angle of attack, as shown in figure roll moment increases with increase of angle of attack regularly till angle of attack 3 and sharply increases till 9degree to reach 0.146, the method reads slop 135.45.

Figure 4.16.b provides a results of rolling moment coefficient for whole missile in transonic flow region (M=0.9) this region of speed represent the region of shock wave and flow variation so the slop of the result decreased compared with previous flow region to reach 95.86.

Figure 4.14.c shows the rolling moment coefficient for whole missile in supersonic flow region (M=2.5) it's Obviously from above figure the roll moment coefficient reveres the direction when increase the angle of attack in supersonic region this because the shock wave is continues in this region (supersonic region).

4.5 Effects of the setting angle (Cant angle):

The side force moment and self-induced rolling moment are extremely important to the coning movement stability of the whole rocket.

Changing the setting angle of the fins can greatly change the corresponding moment coefficients. To study the effect of setting angle, three different geometries were prepared with setting angles (δ=+0.5°, δ=0°,δ=-0.5) figure 4.14(a,b and c) shows the effect of setting angle at M=2.

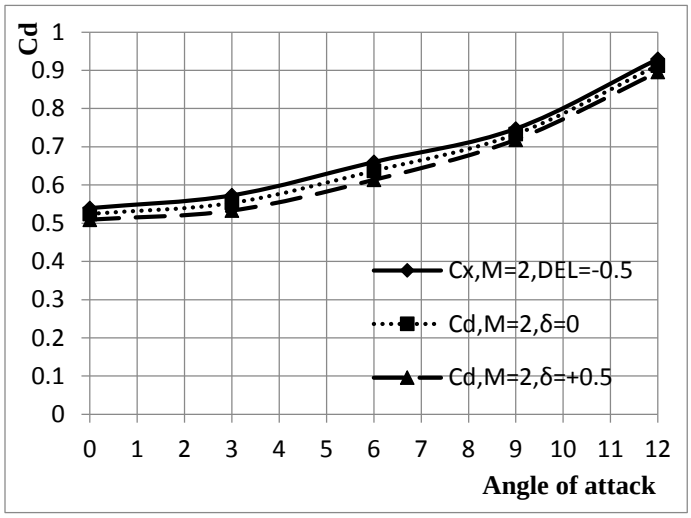

(a)

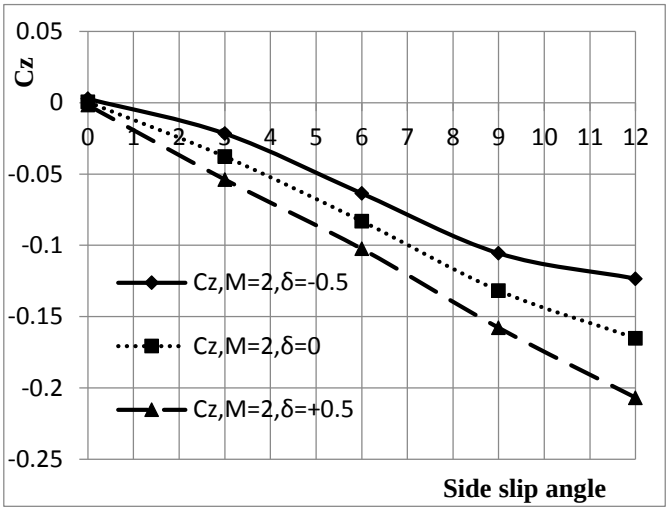

(b)

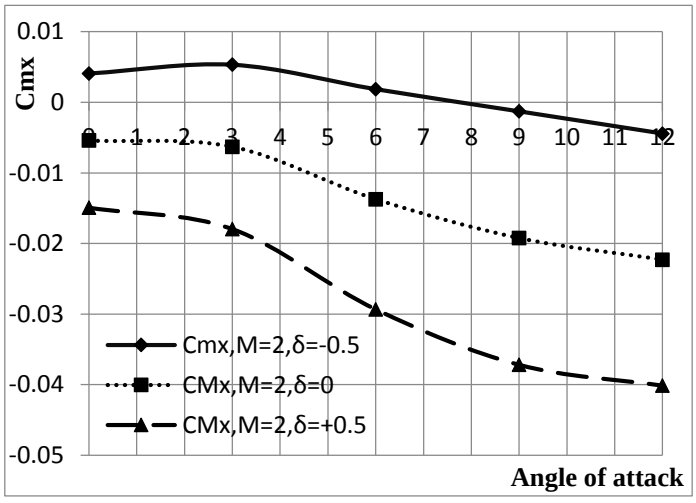

(c)

(c)

Figure 4.17: setting angle at effect at (M=2)

Figure 4.17.a: shows the total drag coefficient for various fins setting angles at supersonic speed (M=2), From the figure it can be seen that negative setting angle generates more drag compare with zero and positive setting angle this, because at the negative setting angle the surface area which faces the airflow is large compared with zero and positive setting angle .and zero setting angle has drag coefficient more than positive setting angle. The computational method at (δ=+0.5°) reads drag coefficient 0.54 while reads 0.52 at zero setting angle and reads 0.509 at (δ = -0.5°).

Figure 4.17.b: illustrates the side force coefficient for different fins setting angle at (M=2), As shown in the figure above by decreasing the setting angles, the corresponding side forces can be greatly increased. Side force coefficient at negative, zero and positive setting angle is 0.0028,0.00059 and -0.00166 at zero angle of attack respectively , where side force coefficient reaches -0.1056,-0.1317 and -0.157 at 9° angle of attack. side force coefficients for negative setting angle is greater than that of the positive setting angle and zero setting angle has side force coefficient more than positive setting angle. This side force has strong effect on rolling moment.

Figure 4.17.c: represents the roll moment coefficient for different fins setting angle at (M=2), it's obvious that, the negative setting angle produces rolling moment coefficients effectively compared with zero and positive setting angles this because it has a large surface area subjected to airflow and the side force also produces roll moment. However, the rolling moment coefficients can reach 0 at the high angles of attack This phenomenon has indicated that at the high angles of attack, keeping a certain negative setting angle can effectively avoid the coning movement and improve the flight stability.

4.6 Flow visualization:

ANSYS(Fluent) software has strong capability to visualize the results of the simulation in different aspects, the below section shows the flow field structure for some flow properties (such as static pressure, dynamic pressure, velocity and density) through different regions of speed. The colors at the left side of the figure indicate the value of flow property in each region of the flow field, the gradient in colors starts from red as a maximum value, and decreases gradually till reaches blue as a minimum value of the property under study.

4.6.1 Missile active phase:

In this section some flow properties will be visualized such as

Figure (4.18.a.b.c) shows the contour of static pressure in different speed flow regions in case of missile active phase .

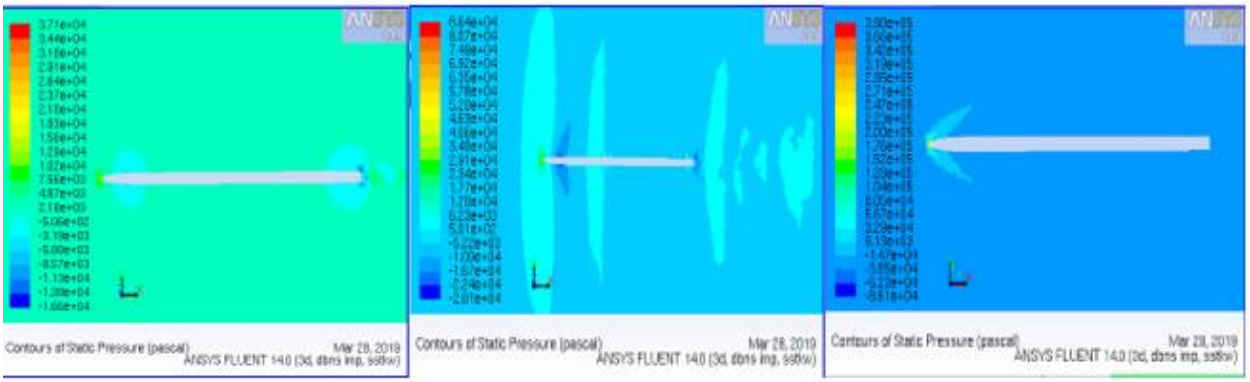

(a) (b) (c)

Figure (4.18) shows the contour of static pressure in different regions of speed

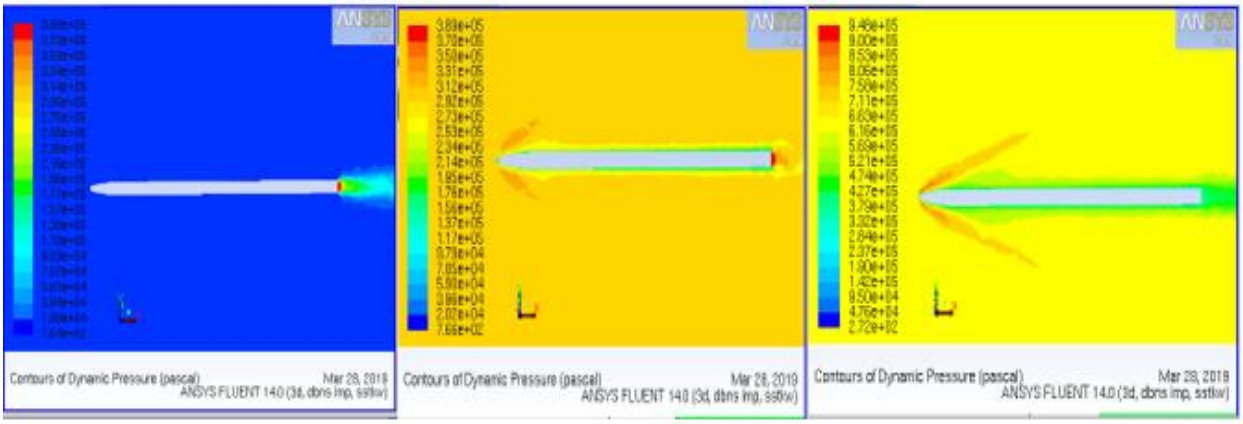

(a) (b) (c)

Figure (4.19) shows the contour of dynamic pressure in different regions of speed

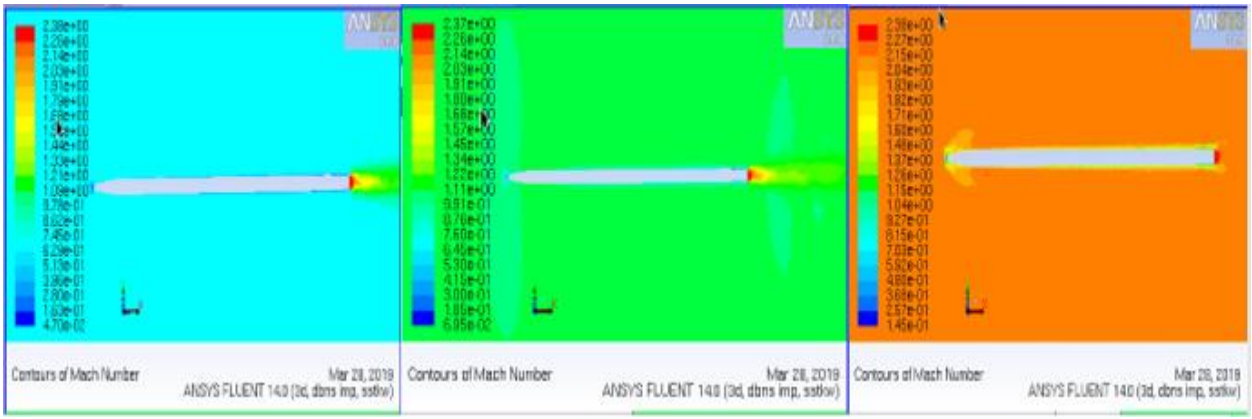

(a) (b) (c)

Figure (4.20) shows the contour of Mach number in different regions of speed

Figure (4.18.a) represents the flow field structure for static pressure in subsonic flow region (M=0.7) It is clear in the figure that the highest value of static pressure is located at the nose of the missile it reaches $3.71 * 10^4$ Pa, which is the red zone, because the nose of the missile represents stagnation area.

Also, there is a change in the static pressure from the nose tip , which decreases in value due to the shape of the nose, and the value of the static pressure is not changed until close to the rear part of the missile The static pressure starts decreasing as a result of the sudden decrease in the diameter of the rocket.

The figure shows that the lowest value for static pressure is in the blast area because it is a very high speed zone it reaches $-1.66 * 10^4$ Pa.

Figure (4.18.b) shows the contour of the static pressure in transonic flow region (M=1) ,it can be seen that the value of the static pressure at the transition speed is also starts to change its value from $8.64 * 10^4$ Pa the nose of the rocket, where the highest value of the static pressure, and at the end of the nose of the missile is $-2.2 * 10^4$ Pa the pressure is very low due to the presence of shock waves in the flow ,and this region represents an area of expansion because the shock wave Always be accompanied by an expansion wave where the speed increases and the pressure decreases (Bernoulli principle).It is also noticed that there is another shock wave in the tail area, but has less strength than the forward wave due to the deceleration of the flow that occurs until the tail reaches.

Figure (4.18.c) reveals the flow field structure for static pressure in supersonic flow region (M=2),from the figure In supersonic velocity zone, the shock wave is still present, but it becomes more oblique and closer to the missile body, which has small wave drag compared to normal shock wave ,the value of static pressure at the nose of the missile is $3.9 * 10^5$ Pa,. It is noticeable from the figure that the shock wave at

the tail area began to disappear at high velocities due to the phenomenon of separation in the flow.

Figure (4.19.a.b.c) shows the contour of dynamic pressure in different flow regions in case of missile active phase .

Figure (5.2.a) illustrates the flow field structure for the dynamic pressure in subsonic flow region (M=0.7) It is observed from the figure that the highest value of the dynamic pressure at the area of the missile's nozzle which reaches $3.71 * 10^4$ Pa,, and less value at the tip of the missile which is $3.71 * 10^2$ Pa, because it is the stagnant flow area.

.Figure (5.2.b) shows the contour of the dynamic pressure in transonic flow region (M=1) ,it can be seen that the highest value of dynamic pressure is $3.89 * 10^5$ Pa, at the missile's nozzle area .At this region of speed the shock is clearly captured at the front part of the missile.as a result of shock wave appeared the dynamic pressure value is very large at the area of shock wave which is $2.92 * 10^5$ Pa, where at the minimum value is $7.66 * 10^2$ Pa at the nose of the missile.

And also the part of the contact flow of the missile's body has a very low dynamic pressure ($1.56 * 10^5$ Pa) because the speed on the surface is very small for the impact of friction and the generation of the boundary layer

It is also noticed that there is another shock wave in the tail area, but has less strength than the forward wave due to the deceleration of the flow that occurs until the tail reaches.

Figure (5.2.c) represents the contour of dynamic pressure in supersonic flow region (M=2), From this figure the highest value of dynamic pressure reaches $9.48 * 10^5$ Pa, at the area of the missile's nose, It is noted that the shock wave at the front is more oblique towards the body of the missile. This oblique shock has less strength

than vertical shock wave. The high velocity causes the phenomenon of separation of the flow, which leads to increased thickness of the boundary layer.

And also the part of the flow contact to the missile body has a very low value of dynamic pressure ($4.74* 10^5$ Pa)because the speed on the surface is very small for the impact of friction and generated boundary layer.

Figure (4.20.a.b.c) illustrates the flow field structure of Mach number in various regions of speed in case of missile active phase .

Figure (4.20.a) reveals the contours of Mach number (velocity) in subsonic flow region (M=0.7) It can be seen that from the figure the highest value of Mach number is 2.38 at the area of the missile's nozzle, because the nozzle accelerates the exhaust gases to produce thrust force ,and less value is 0.047 at the tip of the missile because it is the stagnant flow area.And the Mach number of the flow which near the missile's wall reaches 0.396 .

Figure (4.20.b) represents the contour of Mach number (velocity) in subsonic flow region (M=1) ,as the speed of the missile increases towards the speed of sound ,we must consider the compressibility effect on air. near and beyond the speed of sound small disturbances transmitted to other location in isentropic way . it's remarkable that from the figure the area of nozzle represents high speed region (Mach reaches 2.37),the area near to missile nose has Mach number 0.876 and tail considered as disturbance areas as a results of shock waves appearance.

Figure (4.20.c) illustrates the contour of Mach number (velocity) in supersonic flow region (M=2), From this figure the highest value Mach number is 2.38 at the area of the missile's nozzle, It is noted that the shock wave at the front is more oblique towards the body of the missile. This oblique shock has less strength than vertical shock wave. The high velocity causes the phenomenon of separation of the flow, which leads to increased thickness of the boundary layer.

And also the part of the flow contact to the missile body has a very low value of Mach number because the speed on the surface is very small for the impact of friction and generated boundary layer.

4.6.2 Missile passive phase:

In this section the results of missile with passive phase flow properties will show when then engine doesn't produce trust force, and the missile moves only under inertia force.

Figure (4.21.a.b.c) shows the contour of static pressure in different speed flow regions in case of missile active phase

Figure (4.22.a.b.c) illustrates the flow filed structure of dynamic pressure in different speed flow regions in case of missile active phase

Figure (4.23.a.b.c) represents the contour of Mach number in different speed flow regions in case of missile active phase

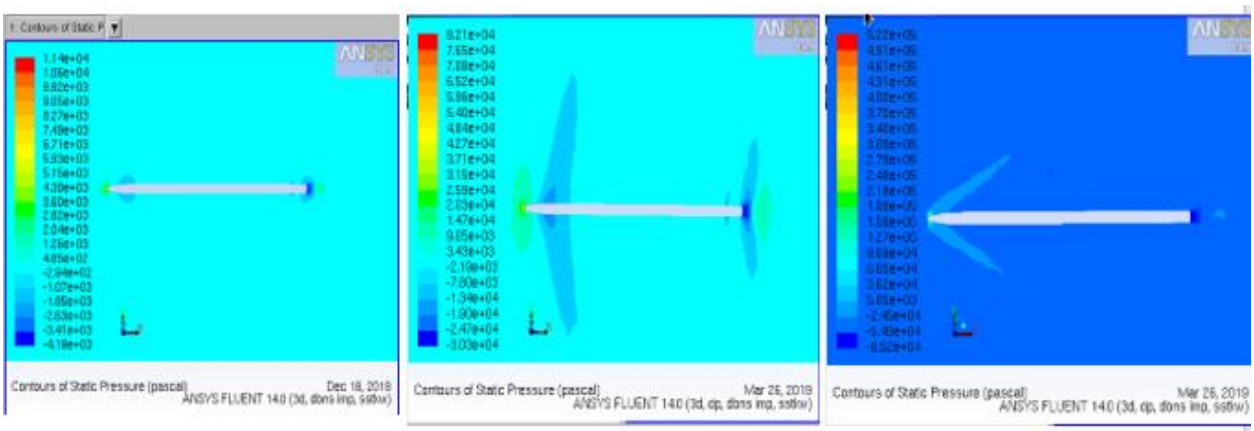

(a) (b) (c)

Figure (4.21) shows the contour of static pressure in different regions of speed

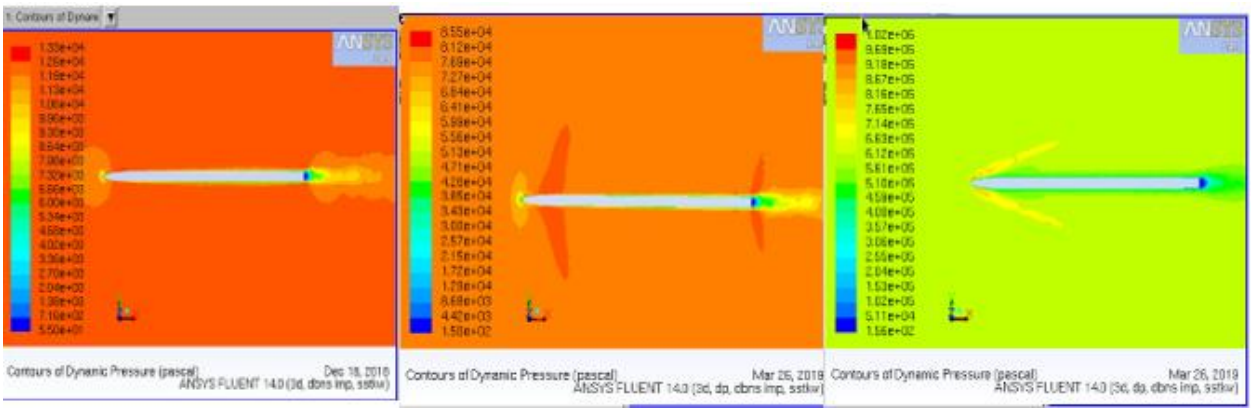

(a) (b) (c)

Figure (4.22) shows the contour of dynamic pressure in different regions of speed

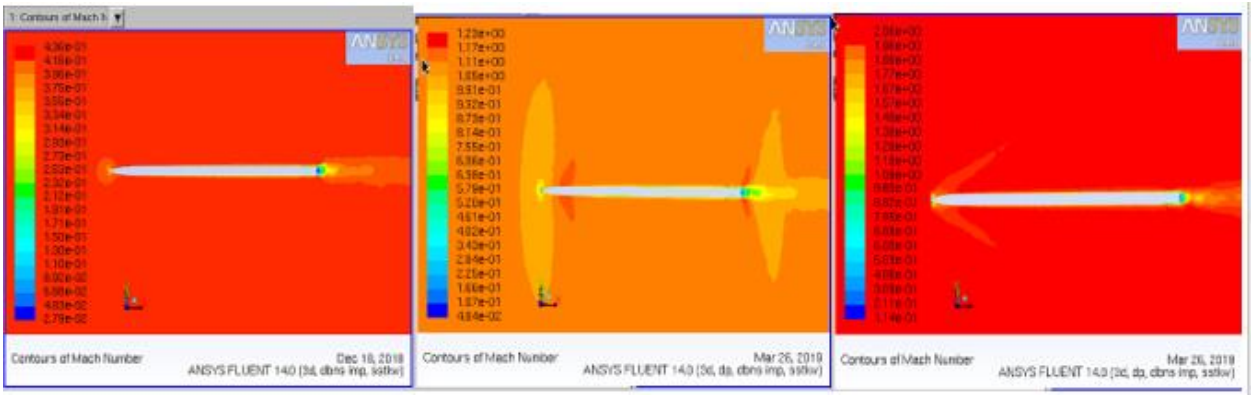

(a) (b) (c)

Figure (4.23) shows the contour of Mach number in different regions of speed

Figure(4.21.a) represents the structure of the flow field of the static pressure in the subsonic flow region (M = 0.7) It is clear in the figure that the highest value of static pressure is located at the nose of the missile, which is the red zone, because the nose of the missile represents stagnation area . The static pressure at the nose is observed to be $1.14 * 10^4$ Pa and as we move towards the rear part there is a decrease and the value at the end of missile's nose is found out to be $1.85 * 10^3$ Pa. After the nose the value of static pressure remains constant, Then it reduces to a value of $-3.41 * 10^3$Pa at the area of the fins ,finally the minimum value of static pressure is observed at the nozzle area which is$-4.19 * 10^3$Pa .

Figure (4.21.b) reveals the contours of the static pressure in the transonic flow region (M = 1) from the figure the highest value of static pressure is $8.21 * 10^4$ Pa it was noted at the missile's nose ,where it reduces to be $-7.8 * 10^3$ Pa at the shock wave area as a result of expansion which accompanied the shock wave ,then at the nozzle area the value reaches $-3.03 * 10^4$ Pa .Also tail shock wave was captured but it has small strength.

Figure (4.21.c) indicates the flow field structure static pressure in the supersonic flow region (M = 2) it can be seen that the maximum value of static pressure is $5.22 * 10^5$ Pa it was noted at the missile's nose ,where it reduces to be $3.62 * 10^4$ Pa at the shock wave area as a result of expansion which accompanied the shock wave ,then at the nozzle area the value reaches $-2.45 * 10^4$ Pa .Also tail shock wave was captured but it has small strength.it is noted that the shock wave becomes more oblique with increase of speed.

Figure (4.22.a) illustrates the flow field structure for the dynamic pressure in subsonic flow region (M=0.7) It is clear that from the figure the maximum dynamic pressure was observed at the area of the missile's nozzle which is $1.33 * 10^4$ Pa, and

it reduces to be $5.5 * 10^1$ Pa at the tip of the missile because it is the stagnation flow area. And also the boundary reduces the speed of the flow contact to the missile's body which leads to make dynamic pressure is low.

Figure (4.22.b) shows the contour of the dynamic pressure in transonic flow region (M=1) ,it can be seen that the highest value of dynamic pressure at the missile's nozzle area it is $8.55 * 10^4$ Pa. At this region of speed the shock is clearly captured at the front part of the missile, as a result of shock wave appeared the dynamic pressure value is very large at the area of shock wave it reaches $5.54 * 10^4$ Pa. tail shock wave was captured ,it is clear that nozzle area and the front of the missile are areas of low dynamic pressure.

Figure (4.22.c) represents the contour of dynamic pressure in supersonic flow region (M=2), From this figure the highest value of dynamic pressure at the area of the missile's nose it reaches $1.02 * 10^6$ Pa, It is noted that the shock wave at the front is more oblique towards the body of the missile. and as we move towards the rear part there is a decrease in the value of dynamic pressure till reaches $1.56 * 10^2$ Pa at the nozzle area. The phenomenon of separation caused by high speed was clear visualized in the flow contact to the missile's body.

Figure (4.23.a) reveals the contours of Mach number (velocity) in subsonic flow region (M=0.7) It can be seen that from the figure the highest value of Mach number at the far field area it reaches 0.436 and it starts to reduce with contact to to the body of the missile where it is 0.253 near the nose and reaches 0.0279 at the missile's nozzle area .

Figure (4.23..b) represents the contour of Mach number (velocity) in subsonic flow region (M=1) ,as the speed of the missile increases towards the speed of sound ,we must consider the compressibility effect on air. The maximum value of Mach

number is 1.23 it was at the end part of the missile's nose and it is 1.17 at the fins area where it 0.048 as a minimum value of Mach number which was recorded at the nozzle area.

Figure (4.23.c) illustrates the contour of Mach number (velocity) in supersonic flow region (M=2), From this figure the highest value Mach number at the far field area which is 2.06 and it reaches 1.96 at the front shock wave area and it reduced to be 0.114 at the nozzle area. It is noted that the shock wave at the front is more oblique towards the body of the missile.

Chapter 5:

CONCLUSION & RECOMMENDATIONS

5.1 Conclusion:

Flow field solutions of GRAD rocket were obtained using the method of computational fluid dynamics(CFD) using the ANSYS/FLUENT program as simulation program for both cases the engine works and the engine does not work. Grids were accurately distributed across the flow field, both near the tip of the nose and at the fin edge the rocket.

The method of computational fluid dynamics (CFD) showed excellent agreement compared with Missile Datcom software results.

The study has adopted three different types of WAFs for the rocket configurations and the single domain technology to investigate the lateral and rolling characteristics of WAFs, including the fins setting angles. Simulations have been performed at Mach numbers from 0.4 to 3 through an angle-of-attack range of about 0° to 12° and at side slip angle range of about 0° to 9°.

The results showed that the wrapped around fins (WAF) configurations can greatly improve the longitudinal stability and enhance the longitudinal aerodynamic characteristics for the whole rocket. The total drag of the whole rocket is mainly stemmed from the body, while the drag generated by the WAF account for only about 18.45 per cent. The extra side forces and rolling moments are due largely to the unequal pressure distributions on both sides of the fins (windward or leeward).

Maintaining negative fins setting angle provides additional side and rolling moments which enhances lateral and longitudinal stability. The lateral and longitudinal stability were investigated.

WAFs configuration provide roll moment even at zero setting angle.

The Missile Datcom software was used to verify and validate the CFD's results and the results comparison showed excellent agreement between the two different methods, Missile Datcom software considered as results validation tool.

5.2 Recommendations for future works:

- Execute wind tunnel test to validate the computational fluid dynamics results.
- Study dynamic derivative calculation.
- Calculate the thickness of the boundary layer and modify the dimensions according to the boundary layer calculation in missile Datcom.

References:

[1] Bernhard, Jim, Porcupine, Picayune, & Post: How Newspapers Get Their Names. University of Missouri Press. p. 126. ISBN 978-0-8262-6601-9. Archived from the original on 19 November 2017. Retrieved 28 May 2016

[2] Sutton, George P.; Biblarz, "Rocket Propulsion Elements", John Wiley & Sons. ISBN 978-0-471-32642-7, Archived from the original on 12 January 2014. Retrieved 28 May 2016

[3] MSFC History Office. "Rockets in Ancient Times (100 B.C. to 17th Century)", A Timeline of Rocket History, NASA, Archived from the original on 2009

[4] Scientific-Technical Review, Vol. LVI, No.2, 2006.

[5] Defence Science Journal, Vol. 59, No. 5, September 2009, pp. 471-484 Ó2009, DESIDOC.

[6] Attapon Charoenpon, Ekkarach Pankeaw, "Method of Finding Aerodynamic Characteristic Equations of Missile for Trajectory Simulation", International Journal of Aerospace and Mechanical Engineering Vol:5, No:9, 2011

[7] Rom. Journ. Phys., Vol. 59, Nos. 3–4, P. 369–381, Bucharest, 2014

[8] Chun-Chi Lia et al (2013), "Study of the aerodynamic characteristic and flight trajectories in a tail fin-stabilized projectile with different shapes", 37th National Conference on Theoretical and Applied Mechanics

[9] Aircraft Engineering and Aerospace Technology: An International Journal 88/1 (2016) 82–96.

[10] H. K. Versteeg, W. Malalasekera, New York (1995), "An Introduction to Computational Fluid Dynamics".

[11] P. A. Henne, California (1990), "Applied Computational Aerodynamics", vol. 125 McIntyre, T.C.; Bowersox, R.D.W. & Goss, L.P. Effects of Mach number

on supersonic wrap-around fin aerodynamics. J. Spacecraft Rockets, 1998, 35(6), 742-48.

[12] Jack N. Nielsen, California (1960),"Missile Aerodynamics".

[13] SMT Sudan, kafouri st, khartoum north Sudan, https://www.machinetools.com/en/companies/25803-smt-sudan

[14] Reynolds, Osborne, 1895: "On the Dynamical Theory of Incompressible Viscous Fluids and the Determination of the Criterion." Philosophical Transactions of the Royal Society of London, A, v. 186, pp. 123-164.

[15] Spalart, P.; Allmaras, S. (1992). "A one-equation turbulence model for aerodynamic flows", 30th aerospace sciences meeting and exhibit, AIAA

[16] Hanjalic, K.; Launder, B. (1972). "A Reynolds stress model of turbulence and its application to thin shear flows" (PDF), Journal of Fluid Mechanics

[17] Wilcox, D. C. (2008). "Formulation of the k-omega Turbulence Model Revisited", AIAA Journal.

[18] http://www.dtic.mil/dtic/tr/fulltext/u2/a548461.pdf